Journal of Hydrology 603 (2021) 127103

Contents lists available at ScienceDirect

Journal of Hydrology

journal homepage: www.elsevier.com/locate/jhydrol

Representing a dense network of ponds and reservoirs in a semi-distributed dryland catchment model

Udinart P. Rabelo [a,*], Jörg Dietrich [b], Alexandre C. Costa [c], Max N. Simshäuser [b], Fernanda E. Scholz [b], Van T. Nguyen [d], Iran E. Lima Neto [a]

[a] Department of Hydraulic Engineering and Environment, Federal University of Ceará, Campus do Pici, 60.451-970, Fortaleza, Brazil
[b] Institute of Hydrology and Water Resources Management, Leibniz Universität Hannover, Appelstr. 9A, 30419 Hannover, Germany
[c] Institute of Engineering and Sustainable Development, University of International Integration of the Afro-Brazilian Lusophony, Campus das Auroras, Rua José Franco de Oliveira, s/n, 62.790-970, Redenção, Brazil
[d] Helmholtz Centre for Environmental Research - UFZ, Department of Hydrogeology, Permoserstr. 15, 04318 Leipzig, Germany

ARTICLE INFO

This manuscript was handled by Sally Elizabeth Thompson, Editor-in-Chief

Keywords:
SWAT
Dryland hydrology
Pond
Reservoir
Hydrological connectivity

ABSTRACT

The mismatch between natural water availability and demand in dryland regions is overcome by reservoirs of different sizes with the purpose of storing water. The increase in population in dryland regions and the consequent growth in water demand expanded the construction of small reservoirs, generating in these regions a dense network of reservoirs, which increases the complexity of modeling these hydrological systems. For dryland watersheds modeling with daily time-step, the horizontal connectivity of the reservoir network needs careful representation in order to achieve acceptable model performance, including cumulative effects of reservoirs. However, the horizontal connectivity of reservoir networks is often less investigated in large-scale catchment models. This work presents an innovative way of implementing the dense-reservoir network into the widely used eco-hydrological model Soil and Water Assessment Tool (SWAT), with detailed representation of large and small reservoirs, and an extensive analysis about the cumulative impact of small reservoirs on the horizontal hydrological connectivity for large-scale dryland catchments. A two-fold cross-validation was used against streamflow at a catchment outlet and against in-catchment reservoir water levels. The model daily performance was acceptable despite the input data uncertainty, with good reliability for peak flow in wet years, for nonflow periods and for the rising limb of the hydrograph. The efforts in the parameterization of reservoirs and aggregation of ponds allowed a better analysis of the hydrological processes and their impacts in the catchment. The results showed that small reservoirs decreased the streamflow, but had a low impact on catchment retention and water losses, with 2% of water retention in wet years. However, the water retention reached 9% in dry years, which may worsen periods of water scarcity in the large reservoirs. The spatial representation of small reservoirs for a high-density network in the SWAT model and the results of the cumulative impact of small reservoirs may be relevant for a better understanding of hydrology in dryland catchments, and can be applied to catchments in similar climatic and socio-economic environments.

1. Introduction

Dryland environments are home to the world's water poorest populations and, during recent decades, have been subjected to increases in population, partial rise in living standards, development of irrigated agriculture, and new activities – especially tourism – that have drastically changed water and land use. These populations are vulnerable to the adverse consequences of environmental changes and in need of regional hydrological studies for better water resources management and water-scarcity risk reduction (Gutiérrez et al., 2014; AghaKouchak et al., 2015; Mallakpour et al., 2018; Samimi et al., 2020; Yao et al., 2020). To overcome the mismatch between natural water availability and demand, dams of different sizes have been built with the purpose of storing large amounts of water during the wet season, which may then be used during the dry season and dry years (Simmers, 2003; Mamede et al., 2012; Mady et al., 2020).

The increase in population in dryland regions and the consequent growth in water demand for human activities expanded the number of

* Corresponding author.
E-mail address: udinart.rabelo@ifce.edu.br (U.P. Rabelo).

https://doi.org/10.1016/j.jhydrol.2021.127103
Received 25 March 2021; Received in revised form 16 October 2021; Accepted 19 October 2021
Available online 27 October 2021

large, medium and small dams distributed along the catchments (Mady et al., 2020; Samimi et al., 2020). The federal and state governments of dryland regions have promoted the construction of large reservoirs, which mainly serve to provide for the water demand of industries, urban regions and large-scale irrigation agriculture (de Araújo and Medeiros, 2013). Additionally, small-scale reservoirs have been used for a long time, mainly in dryland regions, as a complement to meet the water demand of small municipalities, rural communities and farmers. The small-sized and seasonal freshwater system play an important role in reducing inequalities for rural populations, providing sustainable development for rural communities and farmers. Due to their reduced cost and availability of many favourable locations, the number of small reservoirs has increased in recent decades (de Araújo and Medeiros, 2013; Berhane et al., 2016; Yaeger et al., 2017; Habets et al., 2018).

The spatial density of small reservoirs varies across different regions, with catchments in India with 4.2 reservoirs per km^2, Northeastern Brazil with 0.2 reservoir per km^2 and Australia with values between 0.15 and 6.1 reservoirs per km^2, for example. The advances of remote sensing techniques in obtaining important information from satellite images have allowed a better identification of the dimensions and uses of small reservoirs and assessing their global distribution (Lima Neto et al., 2011; Carluer et al., 2016; Mady et al, 2020; Paredes-Beltran et al., 2021). The small reservoirs (medium to micro-dams) are usually built disregarding the potential impact on the water availability of downstream communities. This has led to the generation of a chaotic system, which is referred to as a *high-density reservoir network* (Lima Neto et al., 2011; Mamede et al., 2012; Abouabdillah et al., 2014). On the one hand, such a reservoir network ensures a more equally distributed use of the water resources among the population of the river basin, as it reduces the concentration of water in large downstream reservoirs and enhances an even spatial distribution (Mamede et al., 2012; Fowe et al., 2015; Zhang et al., 2016). This has also positive effects such as decreasing sedimentation in the large strategic reservoirs (Lima Neto et al., 2011; Berg et al., 2016; Mamede et al., 2018), decreasing soil erosion (Abouabdillah et al., 2014) and decreasing the energy demand for pumping (Nascimento et al., 2019). On the other hand, as the smaller dams are also designed to maximize storage and the flow in tributaries is rare, the spilling frequency of the reservoirs is low, increasing hydrological discontinuity (de Araújo and Medeiros, 2013; Abouabdillah et al., 2014; Peter et al., 2014).

The cumulative impact of the small reservoirs on downstream water availability are not simple to estimate because they are not necessarily the sum of individual effects of each small reservoir. These reservoirs may be inter-dependent and the cumulative effect can be greater or less than the sum of the individual effects, depending on their dimensions, uses and locations. (Habets et al., 2018). However, there is evidence that the cumulative impact of the small reservoirs can be considerable, as the inflow to the large downstream reservoirs is reduced (Malveira et al., 2012; de Araújo and Medeiros, 2013; Fowler et al., 2015). Some modeling approaches have been developed to assess the effects of small reservoirs in a basin. Most of them reported a decrease on the annual stream discharge, with a wide range from 0.2% to 36% and decreases in low flow and peak flow (Neal et al., 2002; Schreider et al., 2002; Nathan et al., 2005; Callow and Smettem, 2009; Hughes and Mantel, 2010; Nathan and Lowe, 2012; Fowe et al., 2015; Ayalew et al., 2017; Habets et al., 2018; Zhang et al., 2020).

Most of those models are, however, based on simple mass balance methods developed for dryland environments. Thus, their application in a scenario of increase in the number of small reservoirs should be done with caution, due to specific water use and hydraulic infrastructure patterns. Moreover, despite the importance of the small reservoirs for local needs and their impact on water availability at catchment scale, the small reservoirs have been neglected by water authorities, providing little technical information about them (Fowe et al., 2015; Habets et al., 2018). Reservoir data scarcity hampers, therefore, successful hydrological model application to drylands and semi-arid environments with high-density reservoir networks, which already face both poor monitoring of streamflow and extreme precipitation variation from year to year. The lack of information on small reservoirs characteristics and the difficulty to estimate cumulative impact is a challenge to assess and to model the hydrology in dryland environments.

The incorporation of reservoirs in hydrological models was carried out using simplified approaches in several other studies to assess their impact in streamflow. In WASA (Model of Water Availability in Semi-arid Environments) the reservoirs are grouped into size classes according to their storage capacity, with reservoirs of a smaller size class located upstream of reservoirs of a higher size class, and arranged in a cascade system, with only reservoirs of the largest size class regarded explicitly in the model in daily or hourly steps (Güntner, 2002; Güntner et al., 2004; Mamede et al., 2018). The TEDI (Tool for Estimating Dam Impacts) model also uses as model input the dam size distribution, subdivided into classes, with computations on a monthly basis. TEDI assumes that reservoirs are connected in parallel, and the excess water spilling from each reservoir is directly routed to the outlet of the catchment, disregarding the spatial arrangement of the single reservoirs. Subsequently, the CHEAT (Complex Hydrological Evaluation of the Assumptions in TEDI) tool was developed by Nathan et al. (2005) and included information on the location of the reservoirs on the river network and the network topology, thus differentiating also between sequential and parallel arrangement of single reservoirs (Nathan and Lowe, 2012; Fowler et al., 2015). However, the horizontal connectivity of reservoir networks is often less investigated in large-scale catchment models.

The eco-hydrological model SWAT (Soil and Water Assessment Tool, Arnold et al., 2012) has been applied worldwide for the simulation of catchments, in particular where water extractions and agricultural water management are of major relevance (e.g., Uniyal et al., 2019 with study areas in India, Chile, Vietnam and Germany). Various SWAT applications regarding the hydrology of dryland areas in China, Mongolia, Azerbaijan, Pakistan, Tunisia, Algeria, Mexico and Brazil have been published (Abouabdillah et al., 2014; Bressiani et al., 2015; Ghoraba, 2015; Molina-Navarro et al., 2016; Luo et al., 2017; Siqueira et al., 2016; Sukhbaatar et al., 2017; Sun et al., 2017; Zettam et al., 2017; Santos et al., 2018; Andaryani et al., 2019; Andrade et al., 2019). Despite this, there are few examples of studies (e.g., Zhang et al., 2012; Liu et al., 2014; Nguyen et al., 2017) that investigate the impacts of the combination of reservoirs of different types and levels of operation on catchment runoff using SWAT. In fact, approaches that mimic the effects of a large number of reservoirs in hydrological model structures have rarely been published. To achieve acceptable model performance in dryland watersheds for daily time steps modeling, the implementation of the reservoir network and its horizontal connectivity is fundamental, with detailed representation of large and small reservoirs, enabling a better analysis of their cumulative effects.

This paper investigates capabilities of the eco-hydrological catchment model SWAT to represent dense networks of large and small reservoirs as common for many dryland regions, as well as to gain in-depth understanding of hydrological processes and reservoir storage for *meso*-scale dryland catchments. To accomplish this goal, a detailed approach for dense networks of reservoirs is modeled in the eco-hydrological model SWAT, for daily time steps. A new modeling and parameterization strategy of ponds and reservoirs is developed with detailed representation, focusing on the horizontal hydrological connectivity and the cumulative impact of small reservoirs, together with the parameterization of transmission losses and flood routing based on a modified SWAT version (Nguyen et al., 2018), with a corrected Muskingum subroutine suggested by the authors. The catchment in the SWAT model is evaluated using streamflow and reservoir water level series by a two-fold cross-validation approach. Moreover, a reservoir scenario approach is performed to assess the impact of the large and small reservoirs on the streamflow and storage volume, including different combinations of small reservoir dimensions. The present study not only improves the

understanding of the hydrology of dense reservoir networks but also proposes a modeling approach that can be applied to water resources management in dryland catchments.

2. Materials and methods

2.1. Study area: Catchment

The region for application of the model is a dryland *meso*-scale catchment in Brazil. The Conceição River (catchment area: 3,347 km^2) is located in the state of Ceará in the Northeast of Brazil (Fig. 1). The discharge from the watershed outlet is monitored daily at the Malhada gauging station. The Conceição River is a tributary of the Upper Jaguaribe (*Alto-Jaguaribe*) River Basin (UJB), which is itself a sub-catchment of the Jaguaribe River watershed. The Jaguaribe River flows through the entire state of Ceará disemboguing into the Atlantic Ocean. The study area sits between the latitudes of −6.5 and −7.5. The altitudes in the region vary from approximately 300 to 870 m, with an average elevation of 550 m.a.s.l.

According to Köppen the climate of the region is defined as semi-arid dry and hot ("Bsh") (de Araújo and Medeiros, 2013). It is characterized by a clear distinction between a rainy and a dry season. The rain period lasting from January through May accounts for about 80% of the total annual precipitation, which ranges from 500 to 1000 mm (de Araújo and Medeiros, 2013), amounting to 700 to 800 mm on average (Malveira et al., 2012). The dry season, however, is characterized by water scarcity as the potential evaporation exceeds precipitation by up to four times annually (Gatto, 1999). The prevailing climatic conditions with high interannual precipitation variability cause regular droughts, which may even occur in several consecutive years. Climate data and its pre-processing are presented in the Supplementary Material.

The vast majority of the region is covered by steppe-like savannah (Gatto, 1999). The predominant natural flora is the so called arboreal *caatinga*, a vegetation type found only in the Northeast of Brazil being composed of trees, shrubs and cacti, which are characterized as tropical xerophytic deciduous broadleaved plants (Malveira et al., 2012; Gatto, 1999). The *caatinga* presents a spatially rather continuous vegetation cover only with slight variations in density. The trees have densely branched stems and firm foliage, which dries out and falls off shortly after the rainy season (Güntner, 2002).

Geologically, 80% of the UJB is composed of crystalline bedrock (Eudoro, 2009), which is characterized by shallow overlying soils with low hydraulic conductivity and porosity (Silva et al., 2007). Therefore, the subsurface water storage (vadose zone and groundwater) in the catchment is limited (Eudoro, 2009). Along the principal rivers and tributaries, alluvial depositions may be found composed by young sandy-clayey sediments. These alluvial bodies present rather high permeability (Feitosa, 1998; Feitosa and de Oliveira, 1998; Colares and Feitosa, 1998). Soil mapping and its physical parameters derivation are presented in the Supplementary Material.

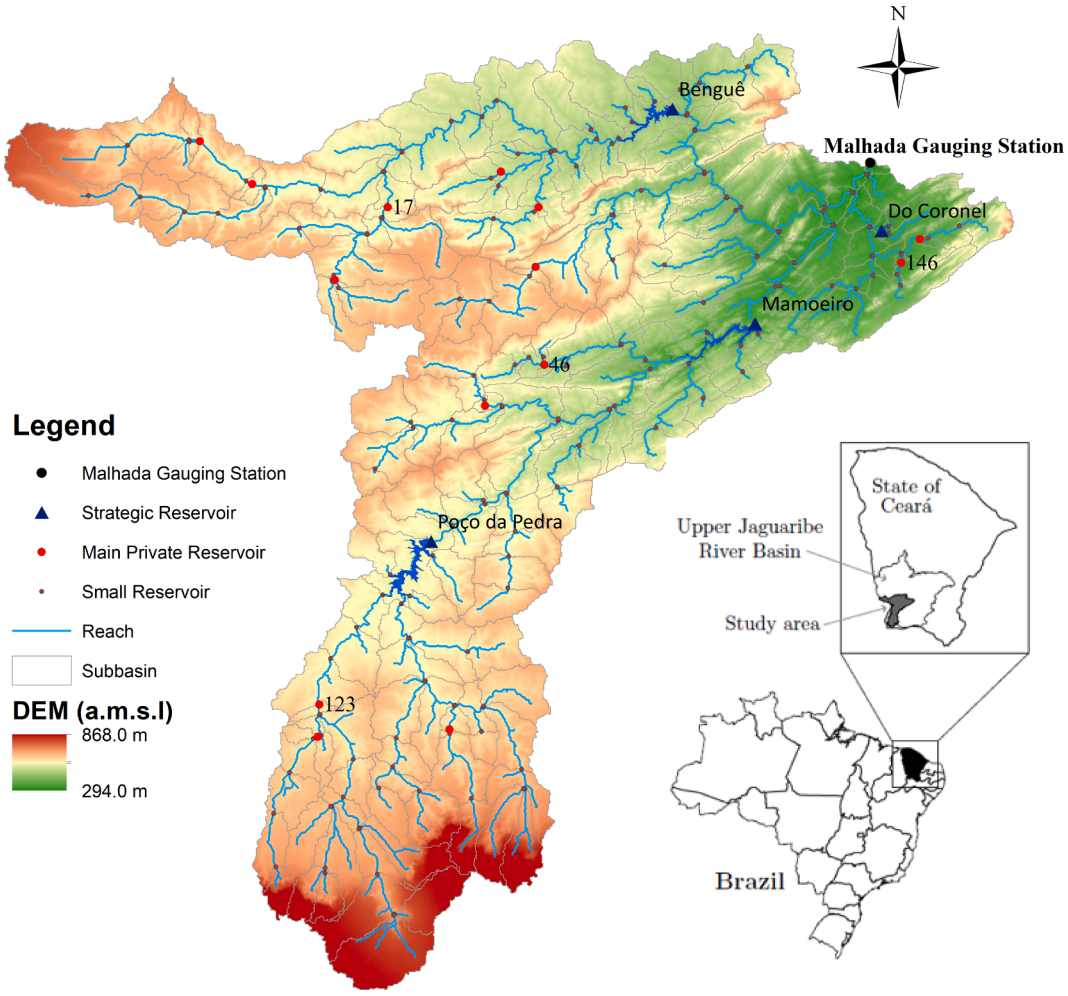

Fig. 1. Location of the study catchment with the main rivers and reservoirs. The numbers 17 and 123 represent the largest main private reservoirs for Benguê catchment and Poço da Pedra catchment, respectively. The numbers 46 and 146 represent the two main private reservoirs with the largest drainage area and the largest storage volume, respectively.

The spatial and temporal variability in rainfall, combined with the low groundwater storage capacity and high evaporation, creates an adverse environment with regard to natural water availability, which is characterized by intermittent rivers and low runoff coefficients (de Araújo and Medeiros, 2013; Malveira et al., 2012). Surface runoff generated in higher parts of the hillslopes is likely to infiltrate into the soil when reaching lower unsaturated areas. If produced at all, streamflow in upstream tributaries is of ephemeral nature, lasting only for short periods (in the range of minutes). Only after several consecutive rainy days, the soil water content is increased so that hydraulic connectivity is established on a catchment-scale and streamflow occurs in the main rivers, continuing over longer periods (in the range of weeks) (de Araújo and Medeiros, 2013; de Figueiredo et al., 2016). In river reaches embedded in an alluvium the flow regime is additionally influenced by channel transmission losses as a consequence of infiltration through the river bed and banks (Costa et al., 2012; Costa et al., 2013).

2.2. Study area: Reservoir system

Reservoirs were distinguished between the large so-called *strategic reservoirs*, constructed and managed by the state government, and the privately built, unmanaged reservoirs of different sizes and shapes (Fig. 1). The latter ones will be generally referred to as *small reservoirs*.

2.2.1. Strategic reservoirs

Four strategic reservoirs, namely Poço da Pedra, Benguê, Mamoeiro and Do Coronel, are located within the catchment (Fig. 1) with a drainage area of 800, 1,062, 1,888 and 25 km^2, respectively (Table 1). The daily storage volume and the flooded area for each strategic reservoir are derived from the monitoring of water levels. The dam constructions usually dispose of two different release facilities (Table 1): a drain unit with an adjustable clasp device and an uncontrolled spillway.

Time series of the controllable releases are available for three of the strategic reservoirs (Poço da Pedra, Do Coronel and Benguê). For Poço da Pedra and Do Coronel, no released discharges occurred for the entire period. The records for Benguê showed some days, during which water was released. No regularity was discernible and the discharges were rather small (usually lower than 100 l/s). As the released discharges are negligibly small compared to the observed streamflow and to the losses caused by lake evaporation (Güntner et al., 2004), they were disregarded for the calculation of reservoir water balance. Differently from the controllable water releases, the spillway overflow is quite relevant to estimate the reservoir water balance, since large flood events were recurrent during the study period.

2.2.2. Small reservoirs

For previous studies on the reservoir network in the UJB (Mamede et al., 2012; Peter et al., 2014), a total number of 230 reservoirs was registered in the Conceição River Catchment analyzing aerial images taken immediately after the rainy season of the three comparatively wet years 2004, 2008 and 2009. This analysis allowed the estimation of the maximum water surface and the corresponding perimeter of the lakes. In-situ measurements of volume, area and height of the small reservoirs are not available.

Table 1
Hydraulic structure of strategic reservoirs located in the study catchment. Data source: Secretary of Water Resources of the government of Ceará (SRH).

Item	Dam Poço da Pedra	Do Coronel	Benguê	Mamoeiro
Operation year	1958	1946	2000	2012
Capacity [hm^3]	52.00	1.77	19.56	20.68
Flooded area at cap. [km^2]	8.320	0.5	3.479	3.691
Spillway type	n. i.	Concrete Sill	Type Creager	Type Creager
Spillway width (constant)	60	24	150	80
Height of spillway crest	22	13	18.54	18
Controllable outlet	yes	no	yes	yes

As the flooded areas represent a moisture state shortly after the rainy season of extremely wet years, it was assumed that they correspond to the maximum capacity, beyond which water is spilled from a reservoir (Mamede et al., 2012; Peter et al., 2014). Hence, an estimation of the storage volumes based on these surface areas was conducted to gain the input data required by the hydrological model. Simplified approaches to estimate the storage capacity and, additionally, the spillway width are shown as follows.

Storage capacity estimation:

Molle (1994) conducted an extensive field study on the geometry of reservoirs in four states of the semi-arid Northeast of Brazil, including the state of Ceará. Based on this work, he developed the following equations describing the relation between surface area, height and volume of a reservoir as a function of two parameters:

$$V = k \bullet h^{\alpha}$$

$$A = k \bullet \alpha \bullet h^{(\alpha-1)}$$

- V: estimated reservoir volume [m^3]
- k: aperture coefficient
- h: reservoir height / water stage [m]
- α shape coefficient
- A: surface area [m^2]

When combining the two equations, one obtains an expression for the reservoir volume as a function of the surface area (Pereira, 2017):

$$V = k \bullet \left(\frac{A}{\alpha \bullet k}\right)^{\left(\frac{\alpha}{\alpha-1}\right)}$$

The two coefficients are site specific and vary depending on the prevailing topography. Molle (1994) determined these coefficients for a sample of 420 reservoirs with capacities ranging from 0.03 to 0.66 hm^3. The mean value of the sample for α and the median for k amounted to 2.7 and 1500, respectively. Using these parameters, the equation has been commonly applied in many studies (e.g. Malveira et al. 2012, Peter et al. 2014).

In order to find mean values for the two coefficients of Molle's equation that are more representative for the reservoir dimensions found in the Conceição River Catchment (reservoirs with flooded area till 0.07 hm^2), which are rather smaller than those from the sample of Molle (1994), a sub-sample of 21 reservoirs from a database published by the Brazilian National Department of Constructions against Droughts (Departamento Nacional de Obras Contra as Secas - DNOCS) (Pinheiro, 2004) was taken at hand. The average value for α, 2.7, and the median for k, 5046, of this sample were determined and adopted for this work. The estimated storage capacity of the small reservoirs detected by aerial images in the catchment, based on Molle's equation, ranges from 2,362 to 1,939,301 m3. The mean and median storage capacity of the small reservoirs are 80,335 and 23,700 m3, respectively.

3. Spillway width estimation:

Not only the strategic reservoirs dispose of spillway structures, but the private non-operated dams as well, even though their flood water release is generated in different manners. The small reservoirs usually have a lowered sill made of compacted soil. Some reservoirs simply spill via a natural or excavated so-called preferential flow channel. No information is available on the width and the height of spillways of small reservoirs. So, in order to realize a broad-scale assessment of the small-

reservoir spillway widths, measurements based on satellite images were conducted in Google Earth in cases where a spillway was clearly discernible from the flight perspective.

After the satellite image analysis, only 21 measurements were considered, because in the majority of cases no clear distinction between dam and spillway was discernible, mainly due to the fact that both structures are made of earth and hence no difference in depth was recognizable. Additionally, some of the larger reservoirs dispose of tubes integrated into the dam, which could also not be assessed in the imagery. Aiming the estimation of all spillway widths, it was assumed that the flood magnitude is related to the upstream drainage area. So, all 21 values of Google-Earth-based spillway width were plotted against the upstream drainage area of each dam obtained from a geographic information system (GIS). After removing three outliers, a linear function was fitted to the plot with a coefficient of determination of 0.88. Based on the thus obtained relationship, the width of the spillway of other small reservoirs could be approximately determined entering the respective drainage area. With this width, the released discharge based on the water stage over the spillway crest may be calculated. However, it must be stated that the relation between width and drainage area represent only a very rough estimation. It presents a source of uncertainty originating from the low resolution of the satellite images in some regions, the potential misinterpretation of them and measuring imprecision.

3.1. Model of the system of reservoirs and ponds

3.1.1. Catchment delineation including reservoirs

For simulating hydrological processes and reservoirs in the catchment, the model SWAT was used. The delineation of the watershed and the definition of its river network (Fig. 1) were done in ArcSWAT based on a digital elevation model (DEM) with 90 m resolution. Outlets of strategic reservoirs were incorporated as nodes. In this section, the model development and parameterization of ponds and reservoirs is presented. Strategic reservoirs and main private reservoirs along the river network were implemented into the SWAT model as “Reservoir” during the watershed delineation, while the other small ones were added as “Pond” as they are situated on tributaries off the main river network (Fig. 1).

The classification of small reservoirs as “Reservoirs” or as “Ponds” was done depending on their impact on the generated water runoff. Water impoundments were implemented as Reservoir, if they meet all of the following criteria:

i. The water impoundment is caused by a dam construction built across the main river reach;
ii. The upstream drainage area of the reservoir is substantially larger than the average design sub-basin area (~20 km^2);
iii. The estimated storage capacity of the water impoundment is >0.01 hm^3.

In the special case that the water impoundment was complying with the first two criteria but not with the third one, it was assigned to the second category (Pond) for means of simplification, even though it was receiving water from upstream sub-basins. By implementing these water impoundments as Pond, as if they were located off the main channel, their water retaining effect was not completely neglected.

To implement the remaining reservoirs as Pond, the following criteria were checked:

i. The water impoundment is caused by a dam construction built across the river reach;
ii. The upstream drainage area of the reservoir is approximately equal or smaller than the average design sub-basin area (~20 km^2).

Fulfilling these criteria, a water impoundment was considered a pond according to the SWAT definition. In case the upstream drainage area was larger than the designated minimum sub-basin area (5 km^2), the outlet was placed on the stream just downstream of the lake, generating a sub-basin whose entire area drains into the pond allocated to it. Deliberately placing certain ponds at the outlet of sub-basins simplifies further calculations for the determination of their drainage fraction, which is a required input parameter for SWAT.

If no dam construction was detected, the water impoundment was disregarded in the model. During a flood event, depressions in the landscape or flood plains may be inundated and filled with water, being registered as a water impoundment through remote sensing. These inundation lakes were neglected in the model as they show different topographic characteristics than the lakes impounded by dams, which would lead to an overestimation of their storage volume when applying the general method for volume estimation from flooded surface area (see section 2.2.2). This would then cause a distorted impact on the surface runoff.

The model catchment delineation ended up with a total of 191 dams and 197 sub-basins (Fig. 1). The average sub-basin size amounted to approximately 17 km^2. A total of 18 dams were implemented as Reservoir (4 strategic and 14 main private) and 79 sub-basins contained dams that were either individually assigned or aggregated as Pond.

3.1.2. Aggregation of small reservoirs into ponds

SWAT allows only one single pond to be allocated to each sub-basin. After the watershed delineation, however, many sub-basins ended up containing multiple small reservoirs, that was considered a reservoir system, in which it was distinguished between a cascade and a parallel arrangement of reservoirs (Fig. 2). In the cascade arrangement, two or more reservoirs are located one behind the other on the same river reach. Water being released from the upstream reservoir will flow into the downstream reservoir. So, the filling of a downstream reservoir depends on the amount of water held up by reservoirs further upstream and thus on the storage capacities and drainage areas of all upstream reservoirs. In the case that two or more reservoirs are arranged parallel to each other, the filling and spilling processes are independent of each other. In the parallel arrangement, each reservoir is located on a separate river branch of the same order. Water being released from one reservoir does not flow into the other. Each reservoir has a separate drainage area.

Based on the arrangement of small reservoirs and their drainage areas, certain calculation rules were applied for the determination of the aggregated reservoir volume. Drainage areas of downstream reservoirs were kept fixed, while the volumes were reduced if necessary. In that way, it was guaranteed that only a fraction of the sub-basin contributes to runoff production that actually does not drain into any reservoir. In the case that a pond is located directly at the outlet, no outflow from the sub-basin will occur until the storage capacity of the aggregated pond is exceeded.

With regard to the rarity and variability of runoff, it is plausible to assume that in some dry years even some of the smaller reservoirs do not spill. So, it was aimed at estimating the mean storage volume that has to be reached so that water is exiting a network of small reservoirs. This volume will be referred to further on as *equivalent capacity*, the system’s impact on the hydrology will be termed *storage effect*.

Two extreme states may be distinguished with regard to the storage effect:

i) The state when the entire amount of generated runoff in the system is stored so that no outflow occurs. This may be seen at the beginning of the rainy season. Only if a certain threshold water volume is exceeded the system spills. This threshold storage may be considered the *effective capacity*.
ii) The other state occurs after full saturation of the system (all reservoirs filled, high soil moisture) after some consecutive rainy days. At

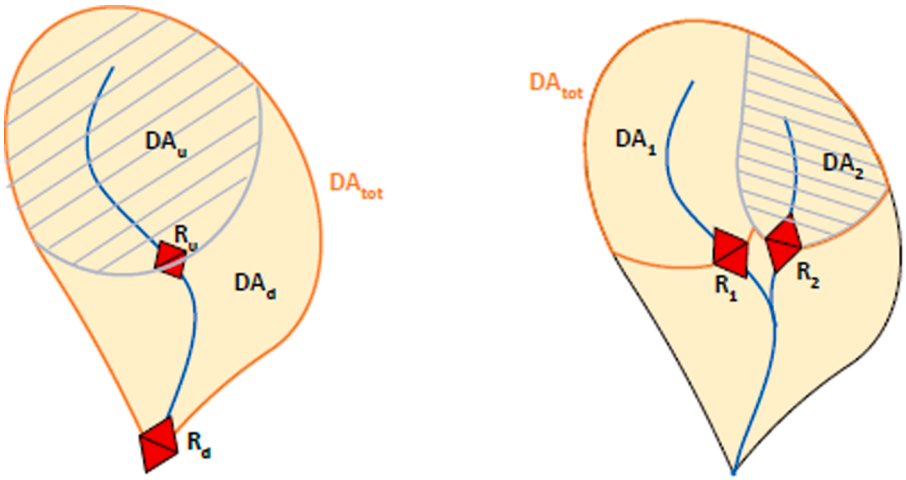

Fig. 2. Schematic illustration of a sub-basin containing two small reservoirs configured in a cascade (left) and a parallel (right) arrangement. DA_{tot}: drainage area of the aggregated pond defining the total drainage fraction of the sub-basin; R_d/R_1 (red squares): downstream/first reservoir; R_u/R_2 (red squares): upstream/second reservoir; DA_d/DA_1 (not hatched): drainage area of downstream/first reservoir; DA_u/DA_2 (hatched in grey): drainage area of upstream/second reservoir; Blue line: river reaches. (For interpretation of the references to colour in this figure legend, the reader is referred to the web version of this article.)

this point, the system only damps the outflow hydrograph, releasing the amount of water above the total storage capacity of the system.

In other words, the effective capacity of the reservoir network determines whether it spills, while the total storage capacity determines how much water is spilled. In order to simulate a storage effect that will match the one in reality on average, it was set the equivalent storage capacity of the lumped pond to a value in between effective capacity and total storage capacity.

If the relation of capacity to drainage area of an upstream reservoir is equal to or smaller than that of the downstream reservoir (considering only the fraction of drainage area beneath the upstream reservoir), the upper dam will spill first. Hence, the equivalent storage capacity of the system amounts to the total capacity, the sum of both. This case corresponds to the assumption of a positively constant relation between capacity and drainage area made for other studies (e.g., Güntner et al., 2004; Zhang et al., 2012). In the case that this ratio is higher for the upstream reservoir, the downstream reservoir will spill first. When assuming the drainage area of the downstream reservoir, though, an addition of the single storage capacities would lead to a strong overestimation of the effective capacity. Spilling from the sub-basin would be simulated with delay or not at all. If only the downstream volume is considered the threshold storage for spilling of the system would be matched but the total capacity would be highly underestimated. In this case, the equivalent capacity is calculated as the sum between the full capacity of the reservoir with the larger specific drainage area and the other capacity reduced by the fraction of the two drainage areas (Eq. (4)).

$$if\ \frac{V(R_u)}{DA_u} \leq \frac{V(R_d)}{DA_d}:$$

$$V_{eq} = V(R_u) + V(R_d)$$

$$if\ \frac{V(R_u)}{DA_u} > \frac{V(R_d)}{DA_d}:$$

$$if\ DA_u > DA_d: V_{eq} = V(R_u) + \frac{DA_d}{DA_u} \bullet \mathrm{V(R_d)}$$

$$if\ DA_u < DA_d: V_{eq} = V(R_d) + \frac{DA_u}{DA_d} \bullet \mathrm{V(R_u)}$$

- V_{eq}: equivalent storage capacity of aggregated pond
- $V(R_u)$: storage capacity of upstream reservoir
- $V(R_d)$: storage capacity of downstream reservoir
- DA_u: drainage area of upstream reservoir
- DA_d: drainage area of downstream reservoir

Accordingly, for a parallel arrangement of small reservoirs in the same sub-basin, if the relation of capacity to drainage area of two reservoirs is equal both will spill at the same time. Hence, the equivalent storage capacity of the system amounts to the total capacity, the sum of both. This case corresponds to the assumption of a positively constant relation between capacity and drainage area.

For the case that this relation is smaller for one of the reservoirs, this dam will spill before the other one. Assuming the sum of both drainage areas as an upstream basin for the lumped pond, the effective storage capacity would be overestimated. Considering only the drainage area and capacity of the reservoir with the smaller ratio the threshold storage for spilling would be matched, but the total capacity would be underestimated. In this case, the equivalent capacity is calculated in the same way as for the sequential configuration, as the sum of the full capacity of the reservoir with the larger specific drainage area and the other capacity reduced by the fraction of the two drainage areas (Eq. (5)).

$$if\ \frac{V(R_1)}{DA_1} \approx \frac{V(R_2)}{DA_2}:$$

$$V_{eq} = V(R_1) + V(R_2)$$

$$if\ \frac{V(R_1)}{DA_1} \neq \frac{V(R_2)}{DA_2}:$$

$$if DA_1 > DA_2: V_{eq} = V(R_1) + \frac{DA_2}{DA_1} \bullet \mathrm{V(R_2)}$$

$$if DA_1 < DA_2: V_{eq} = V(R_2) + \frac{DA_1}{DA_2} \bullet \mathrm{V(R_1)}$$

- V_{eq}: equivalent storage capacity of aggregated pond
- $V(R_1)$: storage capacity of first reservoir
- $V(R_2)$: storage capacity of second reservoir
- DA_1: drainage area of first reservoir
- DA_2: drainage area of second reservoir

By these calculation rules, it was considered that if the combined drainage area is assumed, the storage effect of the reservoir with the larger drainage area is weighted higher for the estimation of the joint storage capacity. In case that multiple small reservoirs are arranged in the same configuration or that the two arrangements are combined in one sub-basin, it was started with the most upstream reservoirs. Their volumes were aggregated according to the respective rule, then this intermediate equivalent volume was again lumped with the small

reservoir further downstream and so on.

3.1.3. Parameterization of strategic reservoirs

In SWAT, a reservoir is basically described by the principal volume (Vpr), the emergency volume (Vem) and the respective flooded surface areas (SApr and SAem). With these parameters the surface-area-volume curve is calculated and the water release is determined. The gradual flood water release from the strategic reservoirs may best be modeled in SWAT with the target release for controlled reservoir function (IRESCO = 2). The outflow routine allows a gradual spilling of the water volume above a certain target volume (Vtarg) and under the emergency volume (Vem). The maximum storage capacity of each reservoir, corresponding to a water level equal to the height of the weir crest, was set as Vpr. Considering that the spillways of all reservoirs in the catchment are uncontrollable free weirs, Vtarg was fixed as Vpr for all months. In order to guarantee a gradual water release over the spillway, Vem must be set substantially higher than Vpr so that it is possibly never exceeded. Vem and SAem are available for strategic reservoirs by the state water agency.

The parameter NDTARG, representing the number of days required for releasing all excess water above Vtarg, determines the amount of water flowing out from the reservoir on each day. It depends on the type and the width of the spillways. In order to find a value for this parameter, daily spillway discharges for different excess volumes were calculated for each strategic reservoir. The discharge over the spillway in SWAT was calculated according to the commonly known weir overflow Poleni equation (Aigner, 2008), which depends on the width and the form of the spillway (Table 1). The weir-type-specific overflow coefficients were set according to the weir types: 2.1 for Benguê and Mamoeiro, 1.75 for Poço da Pedra and 1.6 for Do Coronel. Water levels were considered only up to a height slightly above the maximum observed elevation in the provided time series of the reservoirs: 1 m above the spillway crest for Benguê and Mamoeiro, 0.75 and 0.5 m for Do Coronel and Poço da Pedra, respectively. Excess volumes were also calculated for water stages at 0.01, 0.05, 0.10, 0.25 and 0.50 m above the spillway for all strategic reservoirs.

Therefore, the Poleni equation was solved for half-hourly time steps, readjusting the water stage after each step based on the specific volume-elevation-curve. The amounts of water released after each time step were added up, obtaining the total water volume released in one day. The values for the excess volume, i.e., the volume above reservoir capacity, were then plotted against the values for the calculated released water volume. Linear functions were fitted to the plots (Fig. 3), with NDTARG equal to the inverse of the slopes of the straights. The straight lines presented high coefficients of determination ($R^2 > 0.9$), which led to the conclusion that the spilling behaviour of such reservoirs could be suitably represented by the function implemented in SWAT.

The obtained values for NDTARG reveal that all the excess water is released within slightly more than one day for the reservoirs Benguê and Do Coronel. Mamoeiro spills all the excess water in less than one day. For the excess water to be released from Poço da Pedra, however, it takes more than two days. These statements are only valid for the assumption that no water is entering the reservoir during this time. In reality, the spilling process is much more dynamic. A simulation on hourly time steps would be much more precise, but would lead to high computation time. As the simulation step in SWAT was set to one day due to data availability limitations, the approach presented here was considered the most appropriate way to estimate the daily released water volume.

The parameters IYRES and MORES (year and month, in which the reservoir was built, respectively) were set according to the available information. The parameter EVRSV, the lake evaporation coefficient, was set to 1, which represents the maximum value, to guarantee high evaporation losses. The parameter RES_K represents the hydraulic conductivity of the reservoir bottom. It determines the losses through infiltration. Due to the professional planning and construction of the governmental reservoirs, it was assumed that these dams were sufficiently sealed and RES_K was set to 0.

The initial reservoir volume (parameter RES_VOL) for Benguê was obtained from recorded values shortly after the reservoir became operational in 2000. The initial storage volume represented about 4 % of its capacity. For Mamoeiro, which became operational in 2012, the initial volume was also set to 4 % of its capacity. However, no further time series were available for Mamoeiro. For Do Coronel, the observed storage volume on the first day of simulation in 1979 was obtained from the available records.

The time series for Poço da Pedra showed a gap for the years around

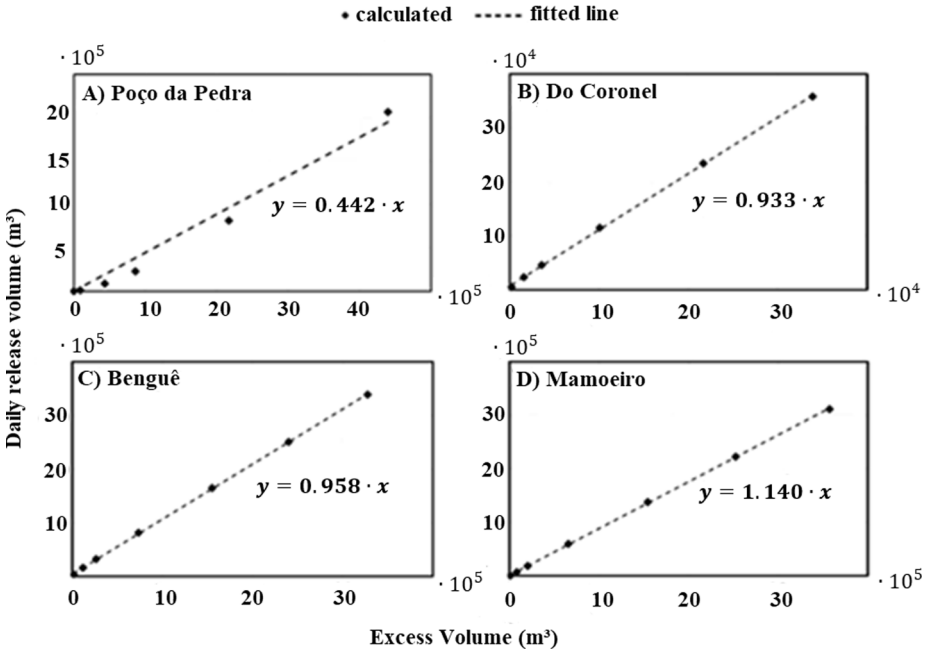

Fig. 3. Excess volumes corresponding to certain water stages (0.01, 0.05, 0.10, 0.25, 0.50, 0.75 and 1.00 m) above the spillway crest plotted against calculated daily released volume with fitted straight line for Poço da Pedra (top left), Do Coronel (top right), Benguê (bottom left) and Mamoeiro (bottom right) Reservoir.

1979. The storage volume at that time was estimated based on all other values registered at the beginning of January in the other years and based on the rainfall measured in 1978. The mean annual rainfall was calculated from five rain gauges inside the study catchment both for the year 1978 and for the entire simulation period. The annual rainfall in 1978 showed to be around 71 % of the mean annual rainfall of the entire simulation period. The average of registered reservoir volumes at the beginning of January amounted to 46 % of the total capacity. So, the initial storage for Poço da Pedra was estimated with these percentages: RES_VOL = 0.71 × 0.46 × capacity. Table 2 summarizes the parameterization of reservoirs, with a description of all parameters.

The representation of the withdrawal of water from the reservoirs was considered in the model in a simplified approach: urban water supply and irrigation were represented by a constant monthly water withdrawal based on state water agency data for each strategic reservoir.

3.1.4. Parameterization of main private reservoirs

Except for the flooded areas measured through remote sensing at the end of the flood season of extremely wet years, no data were available on the 14 main private reservoirs, which were implemented as Reservoir into the SWAT model. As they typically dispose of some type of spillway, it was assumed that the water storage effect of these dams was similar to that of the strategic reservoirs. So, their implementation followed the same principle.

The measured flooded area was set as SApr and the respective volume, which was therefore estimated using the Molle-based approach, was assumed as capacity and set as Vpr. Moreover, the volume corresponding to a water level of 1.5 m above the crest of the spillway was calculated and assumed as Vem. The height of 1.5 m was assumed as a reasonable value for the average height between spillway and dam crest.

Assuming the same procedure of overflow analysis that was followed for the strategic reservoirs and general simplifications of spillway geometric properties, it was found that the excess water is spilled within less than one day for almost all small reservoirs, i.e., less than the model calculation time step. The average NDTARG parameter was set as 1 for the main private reservoirs.

The application *Google Timelapse* was used to determine, in which year each reservoir was built, setting IYRES accordingly. This *Google* function provides satellite images of many regions from the years 1984 until 2017. If it was seen that a dam had been present since 1984, it was assumed that it had been existing since 1979. In these cases, MORES was set to January. In the other cases, MORES was set to November, the ending of the dry season, assuming that the dams are constructed during the dry season.

According to Molle (1989), seepage does not occur in the flooded area of the reservoir due to the underlying crystalline bedrock but rather underneath the dam along the original river bed. In the study, the insufficient sealing and compaction of the dam structures were concluded to be the principal reason for infiltration losses. So, the seepage process implemented in SWAT, assuming a loss through the flooded area (Neitsch et al., 2009), does not adequately represent the infiltration process happening in the field. In order not to neglect seepage losses from small reservoirs, however, the SWAT parameter RES_K (hydraulic conductivity of reservoir bottom) was set according to the average seepage rate found in Molle (1989), which amounted to 2.64 mm per day (0.1 mm per hour). For evaporation losses, the same value of 1 for EVRSV was defined, as described for strategic reservoirs.

Reservoirs that were built during the simulation period were assigned 0 as initial storage volume. For the other reservoirs, the initial storage was set according to the size class (same as used in the studies presented here). Micro-dams (capacity < 0.1 hm^3) were assumed to be empty before the flood season (in January), small-sized dams (0.1 hm^3 $<$ capacity < 1 hm^3) were assumed to be at 10 % of their capacity and the medium-sized ones (1 hm^3 $<$ capacity < 10 hm^3) were assumed to be at 20 % of their capacity. The remaining parameters were left as SWAT default. A summary of the main private reservoir parameters can be found in Table 2.

3.1.5. Parameterization of ponds

The obtained equivalent capacity of a system of small reservoirs was set as the Vpr of the aggregated pond of each sub-basin. The corresponding equivalent surface area was determined according to the same calculation rules, setting it as the SApr of the lumped pond of each sub-basin. With the single reservoir volumes corresponding to a water level of 1.5 m above the spillway Vem and SAem of the aggregated ponds were calculated using the same method.

In SWAT, it is not possible to set the date when a pond came into being. So, it had to be assumed that all ponds had been existing since the beginning of the simulation period, which adds another source of uncertainty considering the transient nature of the micro-dams and looking at the development of dam construction in the region analysed in Malveira et al. (2012).

Based on the considerations made for reservoir bottom percolation, the respective parameter for infiltration through the pond bottom (K_POND) was set as 0.1 mm/h, too. From the investigation about the spilling behaviour, it was found that only above the threshold value of 0.01 for the ratio of capacity to drainage area of the single small reservoirs, it takes more than one day for the excess volume to be spilled (NDTARG > 1.0). From the highest value for NDTARG and the lowest one with the corresponding ratios, a linear relation was set up. Based on this equation the NDTARG parameter was determined for all the small ponds that showed a ratio higher than 0.01. In case the pond was located at the outlet of a sub-basin, the interpolated value for NDTARG was assumed for the aggregated pond in the respective sub-basin. For the remaining sub-basins with ponds, the parameter was set to 1.

Initial storages of the aggregated ponds were also set based on the single small reservoirs located in the sub-basin, following the reservoir-size class as aforementioned. If at least one small reservoir of a higher reservoir size-class (small- or medium-sized dam) is located in a sub-basin, the initial storage was set as a fraction of the capacity of this reservoir, accordingly. Table 3 summarizes the parameterization of ponds.

3.2. Parameterization of dryland hydrology

3.2.1. Model calibration approach

The aim of the calibrated model is to describe the rainfall-runoff relationship of the catchment with the reservoir system as a base for further investigations and scenario simulations. Studying the sensitivity and uncertainty of hydrological parameters is not the subject of this study.

Based on the available data, literature and the experience of the modelers, the following methods were chosen for the calculation of infiltration, evapotranspiration and channel routing, respectively: Curve Number Method, Plant Evaporation Method and Muskingum Method.

The parameters of the model were calibrated with an iterative trial and error procedure with the objective of maximizing statistical model performance and minimizing bias in stream flow, by keeping parameter values in a physically meaningful range. Initial values for the model parameters were derived from field data as much as possible. Then, where field data from the case study area were not sufficient, values from literature about dryland catchments were chosen to represent the characteristics of the study catchment. Finally, remaining sensitive parameters were calibrated.

The model was calibrated separately for the sub-catchments of the three large strategic reservoirs Benguê, Poço da Pedra and Do Coronel. The simulated reservoir volume was compared to the time series for the strategic reservoirs. As the Mamoeiro reservoir became operational only in 2012, after the last year of the Malhada station available time series (1979–2010), it was disregarded for the presented analysis. The remaining sub-basins were sub-divided into three categories: upstream

Table 2
Parameterization of reservoirs (water impoundments implemented into the model as reservoirs). Reservoir numbers and sub-basin numbers correspond to the IDs given automatically in ArcGIS. Abbreviations B., dC., PP. and M. stand for Benguê, Do Coronel, Poço da Pedra and Mamoeiro, respectively.

SWAT parameter		MORES	IYRES [10000 m^2]	RES_ESA [10000 m^3]	RES_EVOL [10000 m^2]	RES_PSA [10000 m^3]	RES_PVOL [10000 m^3]	RES_VOL [mm/h]	RES_K	EVRSV	IRESCO [10000 m^3]	RES_TARG [d]	NDTARGR
Explanation		Month, in which reservoir became operational	Year, in which reservoir became operational	Surface area when reservoir filled to emergency spillway	Storage volume when reservoir filled to emergency spillway	Surface area when reservoir filled to principle spillway	Storage volume when reservoir filled to principle spillway	Initial reservoir storage volume	Hydraulic conductivity of reservoir bottom	Lake evaporation coefficient	Reservoir outflow simulation code	Manually set target volume (equal for each months)	No. of days to reach target storage from current reservoir storage
Res-No.	SB-No.												
2 (B.)	7	8	2000	438.00	2937.00	348.00	1956.00	85.80	0.0	1	2	1956.00	1.04
1 (dC.)	70	1	1979	100.00	300.00	50.00	177.00	46.80	0.0	1	2	177.00	1.08
0 (PP.)	108	11	1979	1639.00	14696.00	832.00	5200.00	1698.00	0.0	1	2	5200.00	2.25
174 (M.)	148	1	2012	454.00	2887.85	369.10	2068.30	82.73	0.0	1	2	2068.30	1.00
13	31	11	1994	22.56	66.91	15.89	38.19	0.00	0.1	1	2	38.19	1.01
17	57	11	2003	40.10	107.62	26.89	57.67	0.00	0.1	1	2	57.67	1.00
19	91	11	1999	23.13	63.44	15.77	34.66	0.00	0.1	1	2	34.66	1.00
24	54	1	1991	7.47	13.66	4.08	5.07	0.00	0.1	1	2	5.07	1.00
30	18	1	1979	21.93	62.36	15.17	34.66	3.47	0.1	1	2	34.66	1.00
32	39	1	1979	12.39	32.56	8.31	17.10	1.71	0.1	1	2	17.10	1.00
34	96	1	1979	10.96	24.59	6.82	11.34	1.13	0.1	1	2	11.34	1.00
46	118	1	1979	89.26	307.50	64.40	192.83	38.57	0.1	1	2	192.83	1.14
90	78	1	1979	14.75	37.03	9.71	18.78	1.88	0.1	1	2	18.78	1.00
123	165	1	1979	20.74	64.12	14.82	37.55	3.75	0.1	1	2	37.55	1.00
128	172	1	1979	4.19	12.91	2.97	7.56	0.00	0.1	1	2	7.56	1.00
146	89	1	1979	45.03	127.57	30.74	71.06	7.11	0.1	1	2	71.06	1.05
197	126	1	1979	8.91	18.15	5.25	7.60	0.00	0.1	1	2	7.60	1.00
203	170	1	1979	5.97	8.26	2.39	2.15	0.00	0.1	1	2	2.15	1.00

Table 3
Parameterization of ponds (water impoundments implemented into the model as ponds). Sub-basin numbers correspond to the IDs given automatically in ArcGIS.

SB No.	Drainage Fraction	Volume Principle (Vpr)	Surface Area Principle (SApr)	Volume Emergency (Vem)	Surface Area Emergency (SAem)	Initial Storage	NDTARG
	[-]	[10000 m^3]	[10000 m^2]	[10000 m^3]	[10000 m^2]	[10000 m^3]	[d]
2	0.1407	7.5238	8.6954	19.8279	16.2424	0	1
3	1	180.773	57.3379	245.2304	71.9404	36	1.35
5	0.4696	0.8167	1.8449	4.2163	5.1859	0	1
6	1	7.5132	9.6866	24.3122	23.3748	0	1
8	0.0391	3.7472	4.8147	10.7188	9.3316	0	1.23
10	0.4067	4.9495	7.3037	13.0763	15.9801	0	1
13	1	5.1694	5.8958	13.3848	10.7323	0	1
19	0.1458	0.8939	2.2837	5.4764	7.2734	0	1
23	0.0763	0.9053	1.9686	4.4619	5.374	0	1
25	1	1.2363	3.0887	7.26	9.4324	0	1
27	1	1.3203	2.4965	5.5348	6.1549	0	1
28	0.6053	1.5654	3.311	7.7935	9.624	0	1
33	1	0.3281	1.0389	2.6666	3.8864	0	1
34	0.3461	1.0677	2.184	4.8947	5.6966	0	1
36	0.2796	2.7783	3.9881	8.7843	8.2325	0	1
40	0.2456	0.2206	0.8092	2.2375	3.4799	0	1
43	1	2.3644	3.6029	7.9147	7.7095	0	1
46	0.8	0.6155	1.2528	3.2769	4.3561	0	1
59	0.8349	1.3593	3.6802	9.2813	12.9686	0	1
60	0.1041	0.1517	0.6393	1.9212	3.1614	0	1
61	1	5.4467	7.7014	17.1033	16.0336	0	1
64	0.3512	13.3103	10.6946	26.894	16.6532	1.3	1
65	1	5.1583	6.819	15.6876	14.6899	0	1
69	1	1.5008	4.0274	9.7324	13.1594	0	1
71	0.3748	1.1897	2.5641	6.0043	7.4319	0	1
72	0.819	1.7086	3.3212	7.5068	8.6277	0	1
74	0.4773	2.6592	4.4424	10.284	9.7641	0	1.22
75	0.0524	0.2017	0.8205	2.4195	3.9328	0	1
77	0.3162	2.9359	5.4036	12.6029	14.5969	0	1
79	0.2002	0.8926	2.127	4.9608	6.3172	0	1.02
80	0.4298	0.2251	1.0437	3.4006	5.8433	0	1
81	0.8215	0.6982	1.7436	4.1308	5.3995	0	1
82	0.7291	0.4968	1.5373	4.1508	6.2157	0	1
85	1	3.6826	4.7623	10.5934	9.2627	0	1
87	0.4025	2.9633	5.2069	11.8974	13.1948	0	1.05
88	0.95	0.7407	1.8059	4.2567	5.5043	0	1
90	1	1.5455	3.1587	7.5267	9.2915	0	1
93	1	7.5586	8.8378	20.4257	17.3195	0	1.02
95	0.7517	0.6823	1.6475	3.829	4.8805	0	1
98	0.4006	1.031	2.8662	7.3597	10.478	0	1
99	0.1782	0.7418	2.1364	5.2665	7.3392	0	1
100	1	29.5171	26.1075	64.7025	45.078	2.95	1.02
102	1	5.2178	7.5602	16.7197	15.8657	0	1
106	1	4.6885	5.7291	12.9448	11.0297	0	1
107	1	16.1602	13.5462	34.7797	24.2638	0	1
110	0.6358	6.8338	7.2609	17.1445	13.7023	0	1.04
112	0.0922	0.3418	1.066	2.7175	3.9329	0	1
113	0.3669	2.3219	5.0349	11.6349	14.25	0	1
117	0.081	4.1549	5.797	12.799	11.7793	0	1
119	0.1587	2.3743	4.6125	10.3382	11.7731	0	1
120	1	6.3861	8.8767	19.733	18.2893	0	1.05
122	1	3.6661	6.3311	14.2447	15.3917	0	1
123	1	4.1293	6.2352	14.076	14.1237	0	1
124	0.9464	2.5164	4.4371	10.3236	11.7177	0	1
128	0.1765	0.3815	1.1425	2.8614	4.0627	0	1
131	0.1025	0.578	1.4841	3.5123	4.6224	0	1
132	0.191	2.0321	4.3421	9.9109	11.9397	0	1
134	1	9.3236	13.8683	31.2845	31.0957	0	1
135	1	31.3789	22.0259	59.2537	34.1384	3.14	1.02
137	0.2512	1.0437	2.5996	6.1387	7.9998	0	1
138	0.1997	0.4126	1.2002	2.9704	4.1595	0	1
139	1	3.279	4.4266	9.7989	8.819	0	1
142	1	3.8062	5.6076	12.4575	12.0347	0	1
144	0.9	0.7818	1.7949	4.1178	5.1092	0	1
149	0.2237	0.1046	0.5058	1.6715	2.8961	0	1
150	0.5671	0.3025	0.9872	2.5698	3.7969	0	1
153	0.1916	25.1365	15.9595	44.4581	22.853	2.51	1.15
154	0.0536	0.0951	0.4765	1.6162	2.8355	0	1
157	0.1087	0.6223	1.8313	4.6474	6.6331	0	1.05
159	1	0.304	0.9902	2.5753	3.802	0	1
168	0.3333	0.7133	1.6942	3.9201	4.9533	0	1.19
171	0.9508	3.1478	4.3143	9.5366	8.6696	0	1

(*continued on next page*)

Table 3 (*continued*)

SB No.	Drainage Fraction	Volume Principle (Vpr)	Surface Area Principle (SApr)	Volume Emergency (Vem)	Surface Area Emergency (SAem)	Initial Storage	NDTARG
	[-]	[10000 m^3]	[10000 m^2]	[10000 m^3]	[10000 m^2]	[10000 m^3]	[d]
173	0.1667	0.2131	0.7918	2.2051	3.4481	0	1
175	1	2.5427	3.7716	8.2931	7.9395	0	1
181	1	2.6293	3.852	8.4747	8.0486	0	1
183	0.0633	5.2966	5.9868	13.6159	10.8486	0	1.07
187	0.0855	0.3322	1.0472	2.6822	3.9006	0	1
193	1	2.8781	4.0776	8.9893	8.3529	0	1
195	1	1.0286	2.1333	4.7922	5.6212	0	1

sub-basins with mountainous river reaches, transition sub-basins with medium-order river reaches and down-stream sub-basins. The sub-division was done by personal judgment with regard to the topography, slope classes and the order of the river reaches.

It is common in hydrological modeling to use warm-up periods, especially when the initial simulation conditions are not known. A warm-up is a sufficient period to run the model to initialize important variables or allow processes to reach a dynamic equilibrium. The complexity of watershed-scale processes impact the length of warm-up periods for hydrological models. However, two to four years are recommended by model developers due to having a complete hydrological cycling in the modeling. These periods are used by SWAT modelers in the arid and semiarid region for hydrological studies (Daggupati et al., 2015; Jajarmizadeh et al., 2017; Zettam et al., 2017; Kim et al., 2018; Carlos Mendoza et al., 2021; Mengistu et al., 2019).

The calibration and validation of the model was performed using the technique of two-fold cross-validation. Considering the first two years as a warm up of the model simulation (1979 and 1980), the first half of the series (1981–1995) was used for calibration, while the second half (1996–2010) was used for validation, obtaining the statistical criteria for both series at the Malhada station. Subsequently, the second half of the series was used for calibration, while the first half was used for validation.

The reservoir volume simulation was evaluated for the whole series, but with a special highlight in the periods when each reservoir spilled out. These periods have a greater importance due to the spillway overflow directly influencing the streamflow at the outlet of the catchment. The simulated and observed time series of the reservoir's volume were overlain and their fitting was visually evaluated.

The years considered in the series for two-fold cross-validation have periods of flood and drought, such as 1985 and 2004 (rainy years) and 1993 and 2005 (drought years). These rainy years were extremely wet years, when all strategic reservoirs spilled out. Beyond these extreme years, the preceding and following years were moderately wet to dry. In this way, the model could be evaluated for different extreme seasons and rainfall events.

For the calibration procedure, the daily simulated stream flow were tried to match the daily observed stream flow at Malhada gauging station, evaluating the plausibility of the magnitude and the duration of the uncontrolled released discharges by reservoirs with regard to the stage-discharge curves (i.e., excess-volume-to-released-volume-curves) developed in this work. To assess the fitting of daily streamflow hydrographs (observed vs. simulated), a combination of three quantitative statistical criteria commonly applied in hydrological modeling was used: the percent bias (PBIAS), the Nash-Sutcliffe-Efficiency (NSE) and the Kling-Gupta-Efficiency (KGE).

3.2.2. *Rainfall-runoff process, flood routing and channel transmission losses*

The dominant vegetation *Caatinga* resembles the vegetation type rangeland. The Manning's roughness coefficient for overland flow for rangeland with 20% vegetation cover was provided in Neitsch et al. (2009). The maximum canopy storage (CANMX) was set to 1.5 mm as the average value for canopy storage in an arid environment stated in Attarod et al. (2015). The parameters SOL_AWC (available water capacity) and SOL_K (saturated hydraulic conductivity) were derived by applying pedo-transfer functions (PTF) based on Brazilian literature for each soil layer (Supplementary Material). Three soil types (Latosol Vermelho Amarelo, Bruno não-Calcio and Litolicos Eu Textura Arenosa) had characteristics of vertic soils. For them, the bypass flow function of SWAT was activated.

For a reach of the Middle Jaguaribe River, Costa et al. (2013) found that at the end of regular/moist rainy seasons, the river becomes a losing/gaining system, with its streamflow being sustained from base flow occurring in the underlying alluvium. The test reach represented a high order river in lower areas. As the principal rivers and tributaries in the study catchment are embedded in layers of alluvium as well, similar effects of streamflow being sustained by backflow from these alluvium bodies may also be expected. Therefore, river reaches were classified into three orders in the model: high order reach, medium order reach, and upstream tributary. SWAT allows to calculate water movement from the shallow aquifer to the root zone, which is controlled by the groundwater "revap" coefficient (GW_REVAP). For the respective sub-basins, the GW_REVAP was set accordingly to different values, decreasing in magnitude with increasing reach order.

According to the findings in Costa et al. (2013), transmission losses increase with increasing discharges due to a higher hydraulic head. In order to include a more appropriate approach for transmission losses on a catchment scale, the parameters CH_K2 (effective hydraulic conductivity of the channel alluvium in main river reaches) and CH_N2 (Manning's roughness coefficient for main channels) were set to different values depending on the topographic position of the sub-basins and the slope classes in the vicinity of the main river reaches.

The calibration of other parameters, such as ESCO (soil evaporation compensation coefficient), ALPHA_BNK (bank flow recession coefficient), ALPHA_BF (base flow recession coefficient), GW_DELAY (delay time for aquifer recharge), GWQMN (threshold water level in shallow aquifer for base flow), REVAPMN (threshold water level in shallow aquifer for evaporation) and TRNSRCH (fraction of the transmission losses partitioned to the deep aquifer) can be seen in a summary in the Tables 4–6. Table 4 presents parameters set for the entire catchment. Table 5 presents parameters set for specific sub-basins of the catchment, with distinction between sub-catchments of two strategic reservoirs and topographic position of sub-basins. Table 6 presents parameters set for

Table 4
Parameterization of calibrated model: Parameters set for the entire catchment.

Entire Catchment	
Calibrated Parameters	**Calibrated Value**
GW_DELAY	12 d and 30 d
CH_K1	5 mm/h to 72 mm/h
TRNSRCH	0.3
OV_N	0.6
CN2	57.34 to 92
CH_N1	0.065
CANMX	1.5

Table 5
Parameterization of calibrated model: Parameters set for specific sub-basins of the catchment. Distinction between sub-catchments of two strategic reservoirs and topographic position of sub-basins.

Item of Distinction	Sub-catchments		Specific Sub-basins			
Calibrated Parameters	Poço da Pedra Catchment	Benguê Catchment	Upstream SB	Transition SB/Medium-order Reaches	Downstream SB/High-order Reaches	Lowlands (incl. Do Coronel Sub-catchment)
	Calibrated Values					
REVAPMN	265	265	265	265	265	265
GW_REVAP	0.15	0.15	0.25	0.15	0.1	0.25
GWQMN	700	700	700	700	700	700
CH_K2	25	19	5	20	72	72
CH_N2	0.05	0.05	0.05	0.05	0.05	0.05
SURLAG	4	4	4	4	4	4
ALPHA_BF	0.8	0.8	0.8	0.8	0.8	0.8
RCHARG_DP	0.25	0.25	0.25	0.25	0.25	0.25
ALPHA_BNK	0.6	0.6	0.6	0.6	0.6	0.6

Table 6
Parameterization of calibrated model: Parameters set for specific zones in the catchment. Distinction between soil types.

Item of Distinction	Soil Type				
Calibrated Parameters	Bruno	Latosol	LitolicosEu	Planosolos	Podisolico-EqEu
	Calibrated Values				
ESCO	0.02	0.02	0.02	0.02	0.02
LAT_TTIME	0	0	0	0	0
SOL_K	PTF results	PTF results	PTF results × 0.8	PTF results	PTF results
SOL_AWC	PTF results	PTF results	PTF results × 1.2	PTF results	PTF results
GW_REVAP	0.1 and 0.15	0.15	0.1, 0.15 and 0.25	0.25	0.1 and 0.15
SOL_CRK	0.3	0.4	0.3	0.01	0.01

specific zones in the catchment, with distinction between soil types.

3.3. Reservoir scenarios

One of the goals of this investigation is to assess the impact of the small reservoirs (ponds and main private reservoirs) on the model streamflow and volume series. As the estimate of those structures was made mainly with the help of aerial images, there is considerable uncertainty in this process.

Thus, in order to investigate different scenarios for the dimensions of the small reservoirs (RES_ESA, RES_EVOL, RES_PSA, RES_PVOL and RES_VOL) and ponds (PND_PSA, PND_PVOL, PND_ESA, PND_EVOL and PND_VOL), their volumes were multiplied by factor zero and the factor ten. These parameters represent areas and volumes that were estimated by the analysis of aerial images in the model (see section 2.2.2). “0 time” means the total absence of small reservoirs and was chosen to show how the model behaves without these small reservoirs. “10 times” means a ten times increase in the aforementioned parameters that represent the volumes of these small reservoirs. With these modifications, the model was run from 1979 to 2010 to assess their impact on the simulation of the streamflow at the Malhada station and of the volumes and the spillway overflows for the strategic reservoirs. We especially evaluated the peak values of the streamflow hydrograph at the Malhada station and the number of days of spillway overflow in the strategic reservoirs.

In addition, another scenario approach was performed to assess the impact of the reservoirs on the simulated streamflow at the outlet. The general influence of reservoirs was performed considering 4 scenarios: (i) considering all strategic reservoirs and small reservoirs (reference); (ii) removing all small reservoirs in the hydrological system, but keeping only the strategic reservoirs; (iii) removing all strategic reservoirs but keeping only the small reservoirs; (iv) removing all reservoirs. The model was run for the whole series with these hypothetical scenarios [(ii), (iii) and (iv)] and the streamflow at Malhada station was compared with the reference scenario (i).

Fig. 4 illustrates the main flowchart of this study, with a summary of all methods applied.

4. Results and discussion

4.1. Simulation of streamflow

The most relevant parameters in SWAT simulations in this study were identified as SOL_CRK, TRNSRCH, CH_K2, LAT_TIME, REVAPMN, GW_REVAP and CH_N1. It is worth mentioning that CN2 showed only low sensitivity even though it was often reported as very sensitive in other catchments. We explain that with the climatic and soil characteristics of the area, where soil moisture and infiltration processes more often underlie extreme dry or wet conditions than elsewhere. In this study, the first two years (1979 and 1980) were considered as warm-up period for adjustment of internal processes (e.g., soil moisture redistribution) that moves from an estimated initial condition to a realistic state. The model performance during the two-fold cross-validation periods was assessed with the three previously presented statistical performance criteria. Table 7 presents the obtained values for each for the calibration–validation periods. These values indicate a good model performance. The analysis of the values for both NSE and KGE attested a good overall fit of the simulated and observed hydrographs at Malhada station. The model simulated streamflow peaks with fairly high accuracy with regard to their dates of occurrence and their magnitudes. When calibrating the model with the first half of the series (1981–1995) the model overestimated streamflow values (highly negative PBIAS) for the second half (1996–2010); when calibrating the model with the second half of the series (1996–2010) the model underestimated the streamflow values (highly positive PBIAS) for the first half (1981–1995).

Fig. 5 depicts the observed and the simulated hydrographs for the calibration–validation periods, while Fig. 6 depicts the log flow duration curve for these periods. For better display, Fig. 7 shows close-ups of hydrographs with a logarithmic scale streamflow for the single years (1985 and 2004) during which relevant discharges were observed. These years were chosen because they represent the wettest years, allowing a full analysis of the hydrograph rising limb, the peak flow and the recession flow. For dry years, with low precipitations, and consequently low flows, the analysis of these hydrograph characteristics would be limited. Fig. 5(a, b), 6 (a, b) and 7 (a, b) present results for 1981–1995 calibration and 1996–2010 validation and (c) and (d) in both figures present results for 1996–2010 calibration and 1981–1995 validation. For Fig. 7, only the first half of the year, the wet season period, is

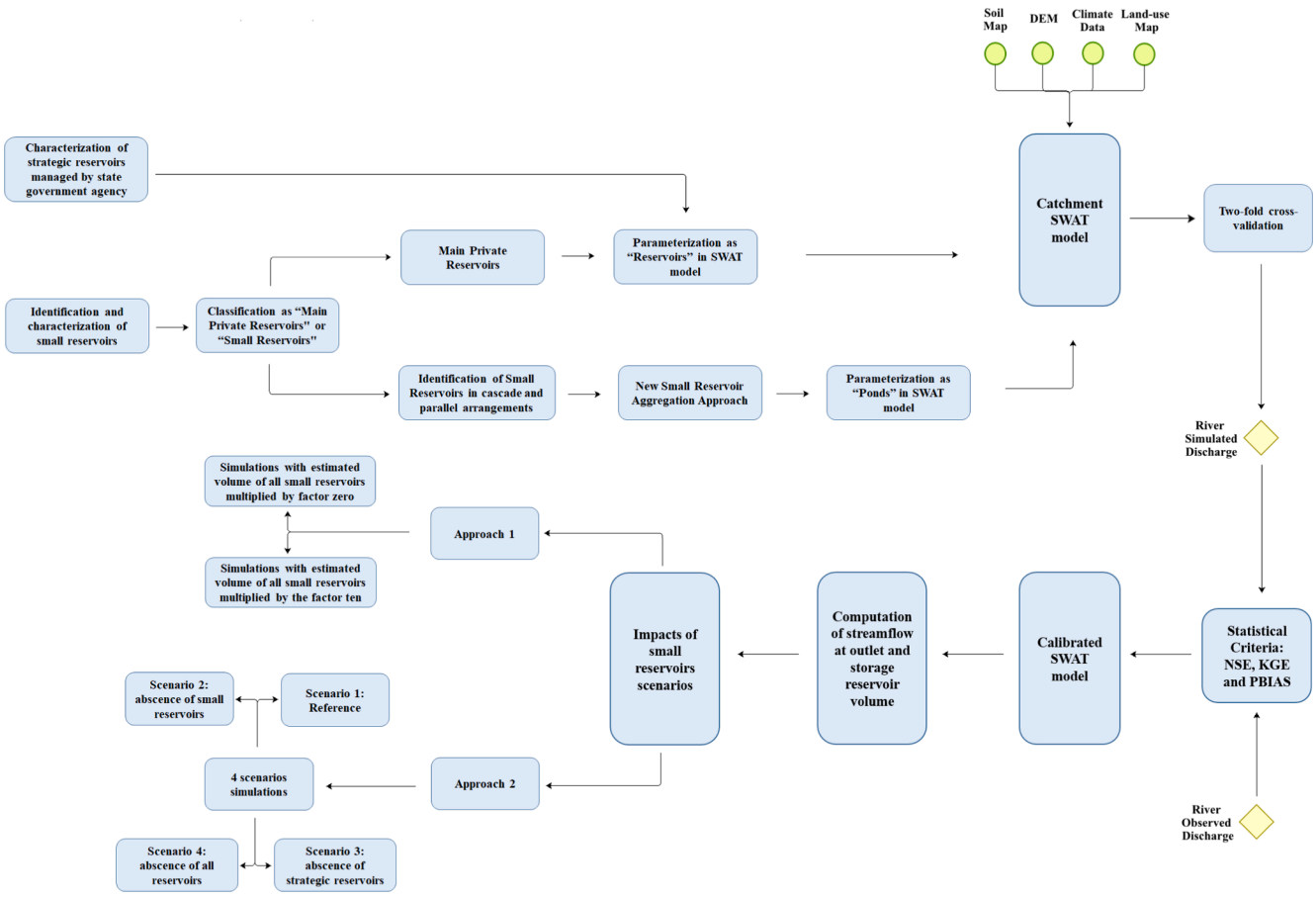

Fig. 4. Flowchart of methods applied in the representation of reservoirs in the SWAT model and in the approaches to impact assessment of small reservoirs in the catchment.

Table 7
Evaluation of model performance in streamflow at Malhada gauging station with statistical methods for calibration period in 2-fold cross-validation of the series, where PBIAS is the percent bias, NSE is the Nash-Sutcliffe Efficiency and KGE is the Kling-Gupta Efficiency.

Performance criterion	Calibration Value (1981–1995)	Validation Value (1996–2010)	Calibration Value (1996–2010)	Validation Value (1981–1995)
PBIAS (%)	5.22	−38.93	2.29	33.55
NSE	0.65	0.56	0.65	0.65
KGE	0.81	0.53	0.82	0.55

presented as for the rest of the year neither observed nor simulated discharges occur (the dry season). It is remarked that the scale of the vertical axis is adapted for each year.

The results show that the model was able to simulate dry years in which no or only minor discharges are registered (1983, 1993, 2001 and 2005) at the Malhada gauging station. For these years no water reached the outlet of the catchment, so the hydrograph was not presented here. This indicates that both the storage capacity of the single reservoirs and the losses due to evapotranspiration and riverbed infiltration were estimated sufficiently high. For years with near-average water yield, the model accuracy was good for some years (1984, 1987–1988, 1990, 1992, 1994, 1996, 1999 and 2003), but was rather poor in others (1986, 1989, 1995, 1997, 2000, 2002 and 2006–2008). For these years with worse accuracy, until 2002 the peak streamflow was underestimated, which means that the observed streamflow has higher peaks and more water reaching the outlet. From 2006 to 2008 the model overestimated the peak streamflow. These results can be seen in Fig. 5. For 2009, the modeled peak was clearly overestimated.

The graphs clarify that for wet years during which the large reservoirs spilled out (1985 and 2004) the days of extreme flood events (high peaks) were matched with high accuracy by the model. The magnitude of the simulated peaks was within a similar range than those of the observed ones. However, the flow recession was not well represented by the model. It was found that it is characteristic for the study area that the streamflow lasted for many days after strong consecutive rain events. The abrupt recession of the simulated hydrograph at the end of wet periods, with streamflow going down to zero just after a few days the peak occurred in all simulation results, while in the observed hydrograph the streamflow lasts for a few days. After extremely rainy periods, water accumulates in the regions close to the river channel, forming flood plains. The river recharge process after this period is notably complex, with unsaturated seepage and vertical unsaturated subsurface water redistribution beneath the stream, lateral stream-aquifer interaction and groundwater flow, parallel to the river course, in unconfined aquifers. These processes and the channel transmission losses for arid and semi-arid watersheds are very simplified in the SWAT model and have a great influence on these basins (Costa et al., 2012).

Some of the years with moderate rain showed worse accuracy in peak streamflow, hydrographs limbs and recession flow, either with underestimation or with overestimation in the simulated values, depending on the year of analysis. Those years with near-average streamflow require attention in the hydrological simulations, mainly due to the possible unsaturated characteristics of the soil. Transmission losses are more complex in these years and the SWAT model equation is relatively simple, depending on hydraulic conductivity, flow translation time, wet perimeter and channel length. Uncertainties in the input data were one of the difficulties during modeling in this dryland catchment, mainly in

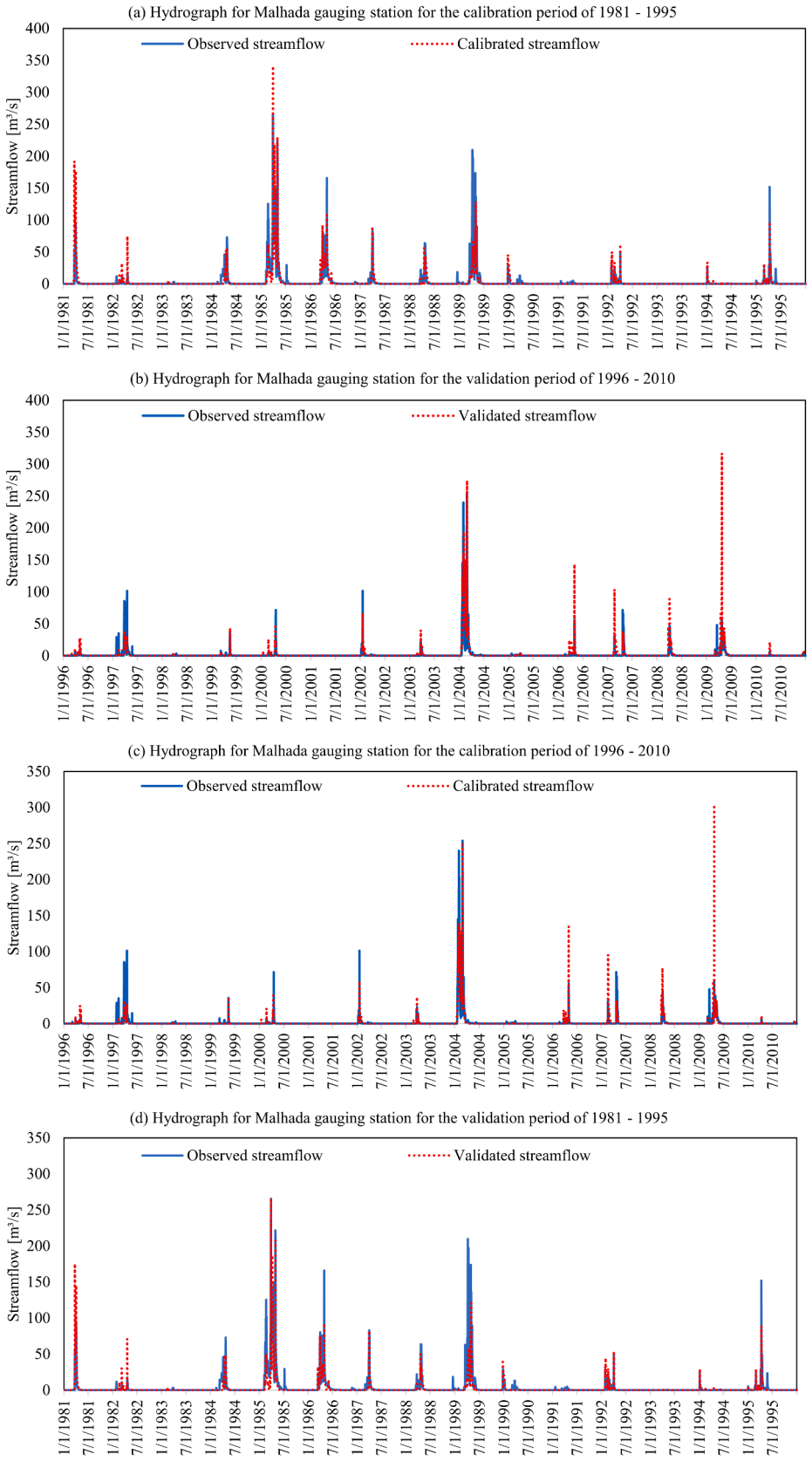

Fig. 5. Comparison of observed and simulated daily discharges at Malhada gauging station for: (a) calibration in 1981–1995; (b) validation in 1986–2010; (c) calibration in 1986–2010; (d) validation in 1981–1995.

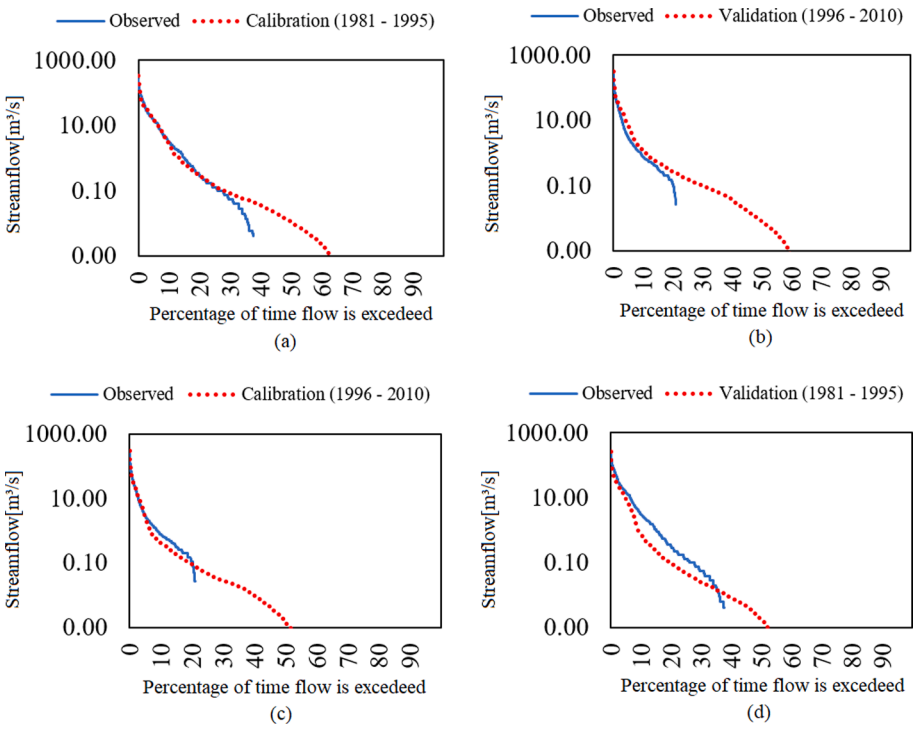

Fig. 6. Comparison of observed and simulated log flow duration curves for: (a) calibration in 1981–1995; (b) validation in 1986–2010; (c) calibration in 1986–2010; (d) validation in 1981–1995.

the values of hydraulic conductivity. The values of hydraulic conductivity and transmission losses estimated also affected the recession flow, whose simulated values also showed streamflow results with sharper drops than the observed values in the hydrographs after the rainy season. In all cases, there is uncertainty in rainfall data (lack of continuous rain gauge monitoring in some days and human errors in measurements) although the 44 stations available in the catchment can reduce errors. No significant errors were found. Despite that, errors of rainfall data during storm events can significantly impact modeling. Even interpolation cannot compensate for gaps in the recording of the local variability of rain.

4.2. Simulation of reservoir volume

The simulated storage volumes during the cross-validation of the three strategic reservoirs Poço da Pedra, Benguê and Do Coronel are presented for comparing their values and temporal dynamics with the observed values based on data availability and operation periods (Fig. 8). From the diagrams, it can be seen that the peaks during flood year 2004 were matched well for the three reservoirs. The model simulated the filling of the reservoir very well until the storage capacity was exceeded. For the other years, the model simulated that the capacity was exceeded for 1986, 1988–1990, 1997 and 2009–2010 for Poço da Pedra, 2006–2009 for Benguê and 2009 for Do Coronel. Analyzing Fig. 8, the storage volume in Poço da Pedra and Benguê reservoirs was higher overestimated in some years, besides the periods that the simulated storage of the reservoir reached the maximum volume (1988–1990, 1997 and 2009–2010 for Poço da Pedra and 2006–2007 for Benguê), when the observed data showed a value quite distant from that. The evolution of the hydrograph, however, was well represented by the model. For Do Coronel, the curve of simulated storage volume showed slightly overestimated values compared to the observed ones for the years after and before the flood years. The overall dynamics is better simulated than for the other two reservoirs.

Despite these differences in storage volumes of Poço da Pedra and Benguê, we did not find any systematic error. The years of 1997, 2008 and 2009, for example, showed considerable streamflow at Malhada gauging station, while the years of 1998, 2001 and 2010 showed low streamflow. There were no direct discharge measurements upstream from the studied reservoirs. Storage volumes were used to validate the reservoir modeling approach. On the other hand, from 2008 to 2010 the model overestimated the storage volumes in Poço da Pedra, as well as the streamflow at Malhada gauging station in these years, especially in 2009. Some characteristics of dryland environments cause uncertainties for modeling of rainfall-runoff processes, for example the nonlinear behavior of runoff generation and the irregular spatial patterns of soil properties (Rödiger et al., 2014; Mamede et al., 2018).

The fall of the storage volume during the dry period, too, was modeled very realistically. For the years before and after a flood year, the curves fitted very well for reservoirs. The slope of the curve after a rainy season was a little more pronounced in the model. This period is characterized by intense evaporation and a decrease in the volume of the reservoirs for semiarid sub-basins and the parameter that calculates the evaporation (EVRSV) in the reservoirs in the model was established at the highest possible value (see Table 2).

The catchment of Benguê reservoir was modeled by Mamede et al. (2018) using the WASA-SED model (Güntner et al., 2004; Bronstert et al., 2014) for the period 2000–2012. The WASA-SED model also simulates the impact of the small reservoirs on the generated catchment runoff as aforementioned. The WASA-SED results for the storage volumes of the Benguê reservoir were very similar to those produced by the SWAT model presented here, although the WASA-SED model was specifically adjusted only for the Benguê catchment.

Furthermore, it can be seen that the model simulated the release from the reservoir during flood events within the calibration and validation periods (Fig. 9). Both the durations and the magnitudes of the overflow discharges seem plausible for all reservoirs. According to the specific stage-discharge curves edited for this study the simulated maximum discharge from Poço da Pedra corresponds to a water stage of about 60 cm above the spillway crest. The maximum simulated overflow discharge from Do Coronel would cause the water stage to reach a height of 40 cm above the spillway crest. The maximum discharge from Benguê

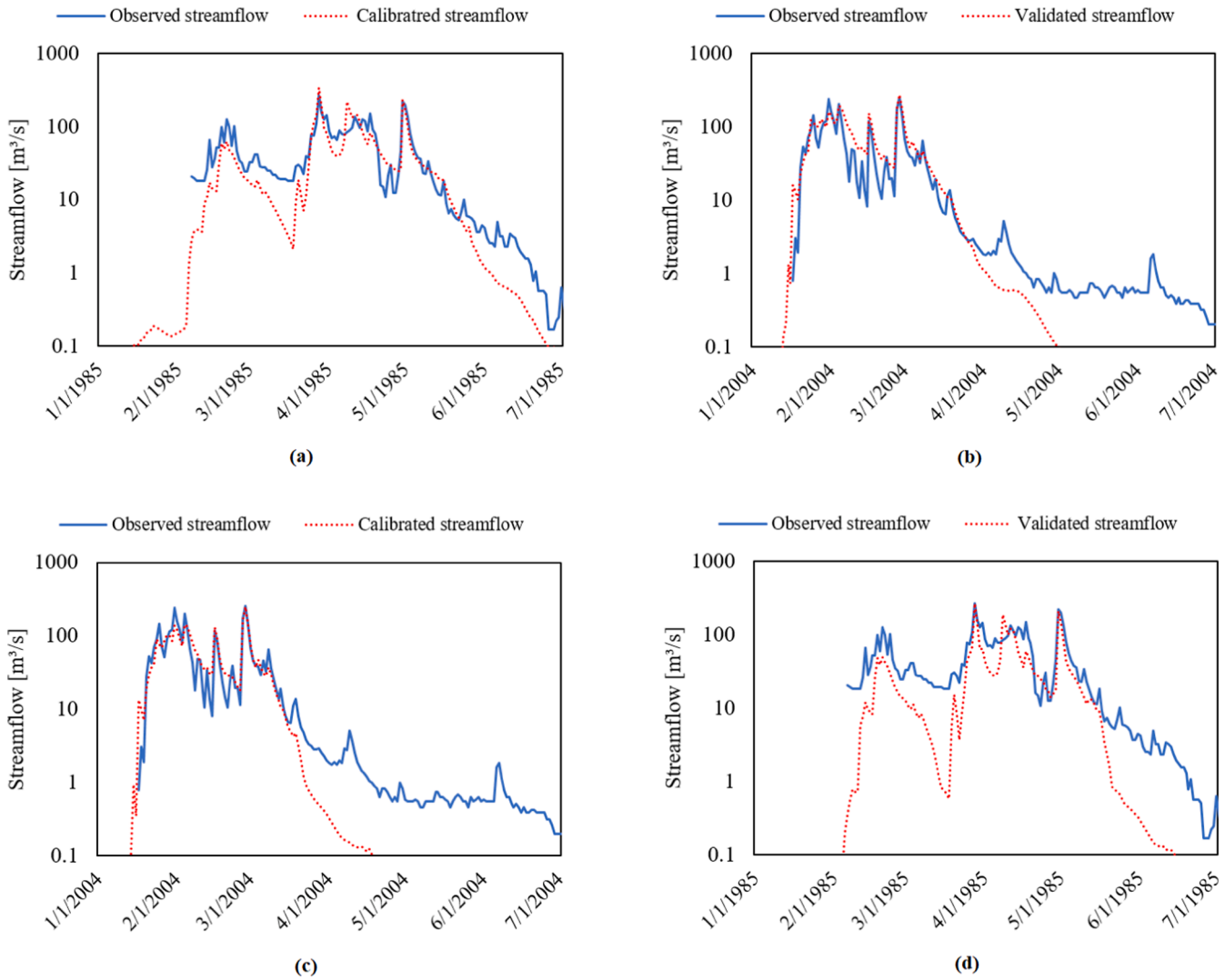

Fig. 7. Comparison of observed and simulated hydrograph for daily discharges at Malhada gauging station for: (a) calibration year of 1985; (b) validation year of 2004; (c) calibration year of 2004; (d) validation year of 1985.

corresponded to a water stage higher than 2 m above the spillway crest. 2.1 m is given as the maximum water level above the spillway. So, in this case it may be assumed that the model overestimated the outflow. But as the outflow from the spillway represents a dynamic process, depending on hourly flood events, the water stage may be kept constant during a longer time span, leading to higher discharges than the one predicted by the stage-discharge curves, which assume no further inflow to the reservoir. As no information was available regarding the spillway overflow from the reservoirs, no further comments on the plausibility of the outflow hydrographs were done. However, the results were an indication that the filling and emptying processes in reservoirs may be mimicked realistically with the SWAT model even on a daily time step, which was rarely shown before.

Beyond the results presented for reservoirs, an analysis was also made for the number of days on which the three reservoirs overflowed. These results were taken from analysis of the simulation, counting the days when each reservoir exceeded capacity resulting in spillway overflow during the simulation period (1979–2010). These values were compared with the number of spillway overflow days from the state water agency observed data for each reservoir. The results were presented in Table 8. The model greatly overestimated the number of days with spillway overflow, mainly for Poço da Pedra and Benguê. This is an expected result, since the hydrographs of these reservoirs for model simulation had several years reaching their capacities. On the other hand, for Do Coronel the results were very close. A greater number of days of spillway overflow from the reservoirs implies that more water reaches the outlet of the catchment, increasing the simulated streamflow values. This could be clearly seen in 2009, where all reservoirs overflowed and, consequently, the simulated peak flow at the Malhada station was much higher than the observed peak flow. Other years that also had simulated streamflow rates greater than those observed (2006, 2007, 2008 and 2010) coincided with the overflow of the reservoirs having a higher number of days in these years.

Fig. 10 depicts the outflow hydrographs for four selected main private dams implemented as reservoirs for the entire simulation period (1979–2010). The two main private reservoirs with the largest drainage area and the largest storage volume (No. 46 and No. 146 respectively) and the largest main private reservoirs for Poço da Pedra catchment (No. 123) and Benguê catchment (No. 17) were chosen for presentation (see Fig. 1), as they had the highest hydrological impact. The diagrams showed that water release from the reservoirs 17, 46 and 123 was simulated by the model only in some years, with the spilling lasting only for a couple of days. As presented before, it was expected that such medium-sized reservoirs spill out only in wet years after consecutive strong rain events. These results agree with this field observation. Hence, the spilling behavior seems realistic. With regard to the spillway

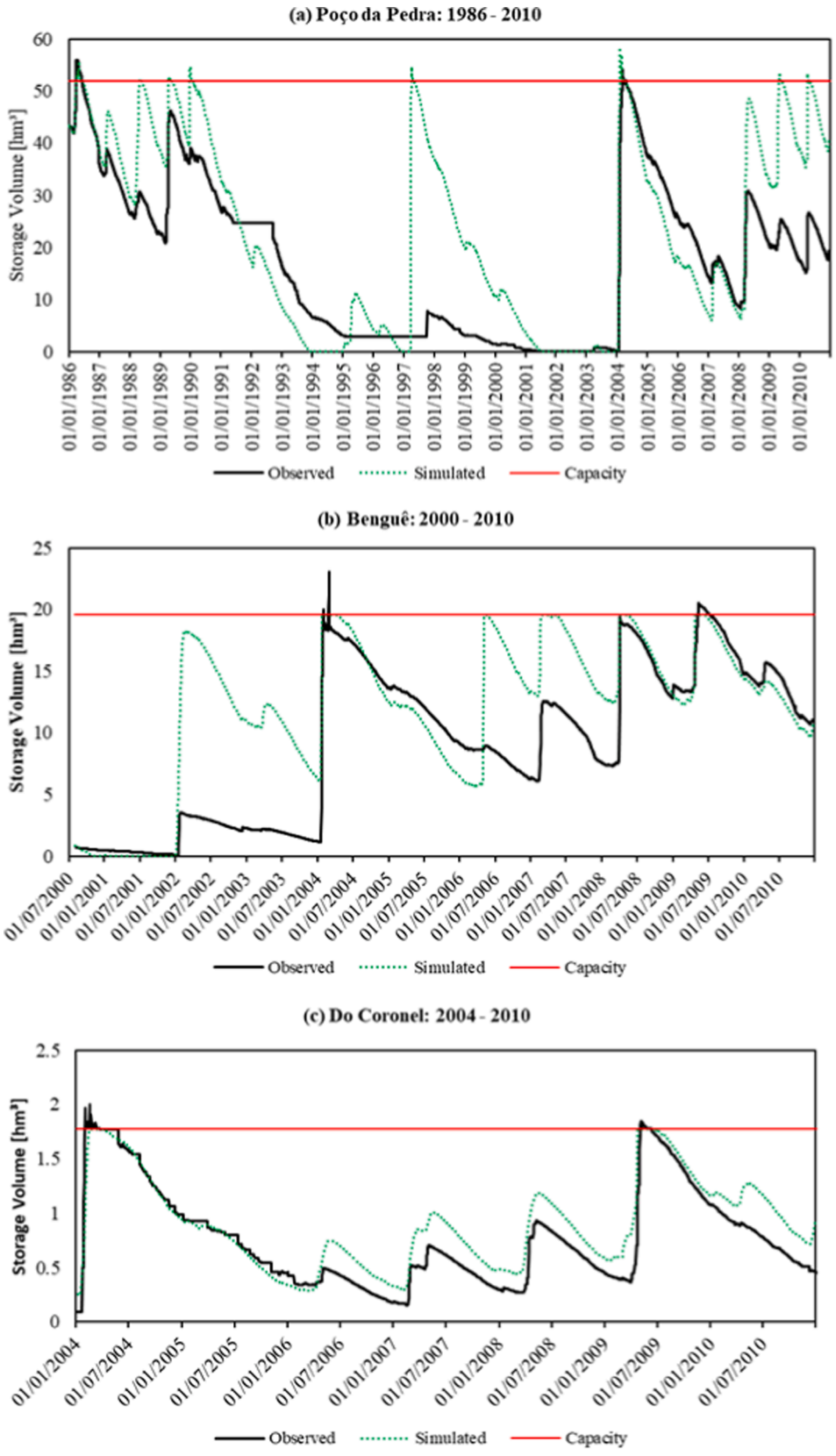

Fig. 8. Comparison of observed by state water agency and simulated by SWAT daily storage volumes in the three strategic reservoirs for the calibration and validation periods: (a) Poço da Pedra (storage capacity 52 hm^3, simulation 1986–2010) (b) Benguê (storage capacity 19.56 hm^3, simulation 2000–2010), (c) Do Coronel (storage capacity 1.77 hm^3, simulation 2004–2010).

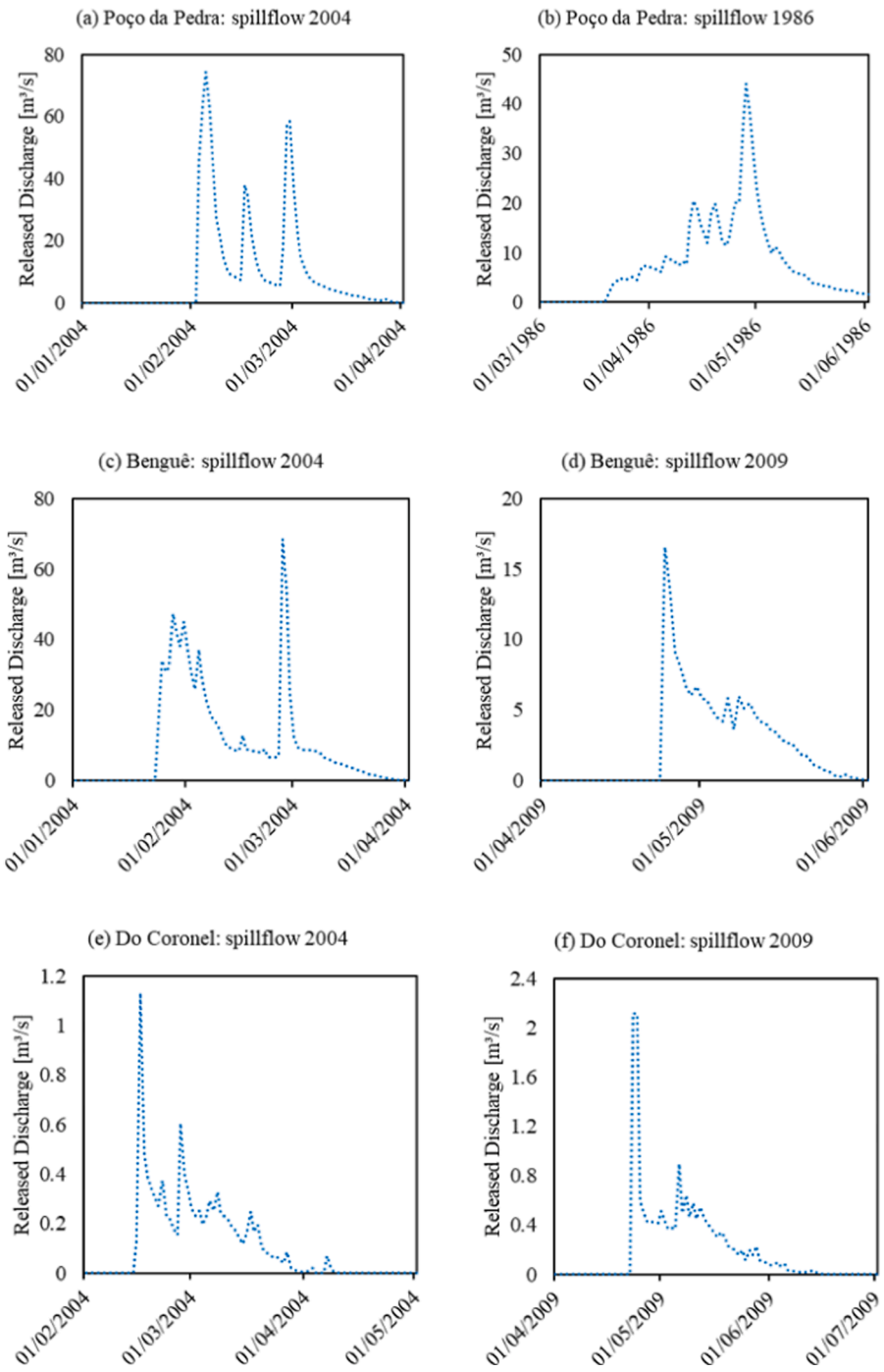

Fig. 9. Hydrographs of released discharge for simulated outflow over the spillway of the three strategic reservoirs for model simulations: (a) Poço da Pedra – 2004; (b) Poço da Pedra – 1986; (c) Benguê – 2004; (d) Benguê – 2009; (e) Do Coronel – 2004; (f) Do Coronel – 2009.

Table 8
Comparison between the number of days with spillway outflow for observed data and the number of days with spillway outflow for model simulations during periods with data availability for reservoirs: 1986–2010 for Poço da Pedra, 2000–2010 for Benguê and 1998–2010 for Do Coronel.

Reservoir	Number of days with spillway outflow observed	Number of days with spillway outflow simulated
Poço da Pedra	97	316
Benguê	64	231
Do Coronel	93	110

outflow simulated for these main private reservoirs, the magnitude of the discharges were consistent considering the smaller drainage areas and the spillway widths estimated. Consequently, it may be stated that the estimation of the reservoir capacity and the model parameterization were reasonable. No other information nor observed data was available for these reservoirs. Therefore, the plausibility of the results may not be assessed more specifically.

The higher frequency and duration of spilling of reservoir number 146 simulated by the model were due to the fact that the soil type present in that area does not have any cracking potential. Therefore, the soil was saturated faster and more runoff was generated leading to a faster filling of the reservoir. As the spillway outflow magnitudes were

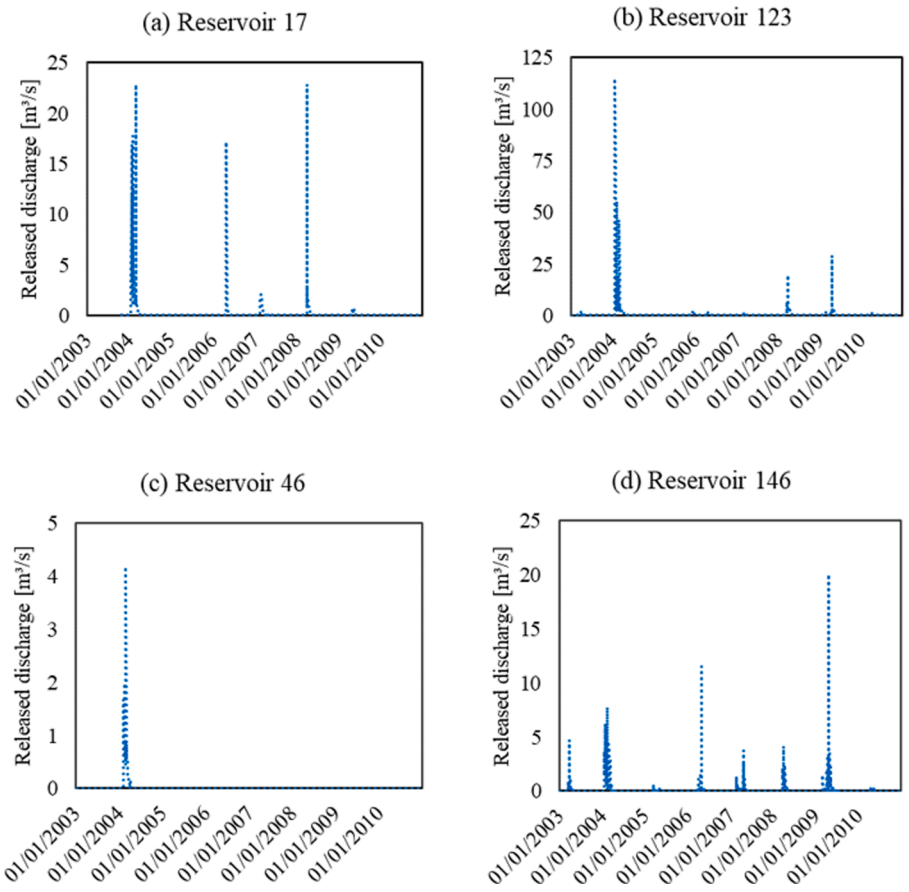

Fig. 10. Hydrographs for simulated daily discharges released from the private reservoirs No. 17 (a), No. 123 (b), No. 46 (c) and No. 146 (d) via spillway for the years 2003–2010.

consistent to the drainage area and the spillway width and the parametrization was based on the calibration of the volume of Do Coronel reservoir located nearby, it may be assumed that these results, too, were reasonable.

4.3. Impact of the reservoir network on streamflow and reservoir volume simulations

The influence of reservoirs on the outflow of the catchment was first investigated with the following four scenarios for the whole flow series (1979–2010): (i) considering all strategic reservoirs and small reservoirs (reference); (ii) removing all small reservoirs in the hydrological system, but keeping only the strategic reservoirs; (iii) removing all strategic reservoirs but keeping only the small reservoirs; (iv) removing all reservoirs. Table 9 presents a comparison for the model results criteria (PBIAS, NSE and KGE) between the four scenarios. The analysis of the statistical criteria in Table 9 showed that removing strategic reservoirs significantly reduced the PBIAS, which means an increase in the simulated streamflow in the outlet. Also, NSE and KGE decreased. This result is in line with the expectations due to the decrease in retention by removing the reservoirs.

Table 9
Comparison of model results in streamflow at Malhada gauging station for different reservoir scenarios (1979–2010).

Performance criterion	Scenario (i) (reference)	Scenario (ii) (only Astrategic reservoirs)	Scenario (iii) (only small reservoirs)	Scenario (iv) (no reservoirs)
PBIAS (%)	0.53	−2.76	−16.99	−20.30
NSE	0.63	0.61	0.51	0.48
KGE	0.81	0.80	0.70	0.66

Besides that, to illustrate the results obtained for wet years, the year of 2004 was chosen to show the comparison between the simulations, with the streamflow in the outlet at logarithmic scale (Fig. 11). The streamflow hydrograph showed that, during the first increasing limb, the scenarios had a similar slope, but the scenarios (iii) and (iv) reached a higher peak flow. Scenarios (iii) and (iv) do not have strategic reservoirs, therefore water retention was lower in the catchment. After this point, all the scenarios showed similar results. As the differences between scenarios (i) and (ii) and between scenarios (iii) and (iv) were very small, this result also showed that the presence of small reservoirs did not significantly alter the streamflow during the rainy season. The water retention due to small reservoirs in wet years was 2%. The decreasing limb and the recession flow showed the same aspect observed in model calibration, with the end of wet periods to be abrupt, with streamflow going down to zero faster than the observed values, probably due to river-aquifer interaction processes that were not catched by SWAT as aforementioned. This behaviour is also seen in other wetted years, such as 1985 and 2009 (not shown here). Therefore, these results indicated that the basin under study is far from reaching its maximum water reserve capacity, especially considering the saturation of small reservoirs.

All scenarios overestimate the observed streamflow data, which can be seen more clearly on the cumulative streamflow representation (Fig. 11). For the scenarios (i) and (ii), during the intermediate rainy season, the simulated recession flow was higher than the observed one, mainly from 02/2004 to 03/2004. Furthermore, the scenarios (iii) and (iv) reached a higher peak flow at the beginning of the rainy season, due to the absence of the strategic reservoirs.

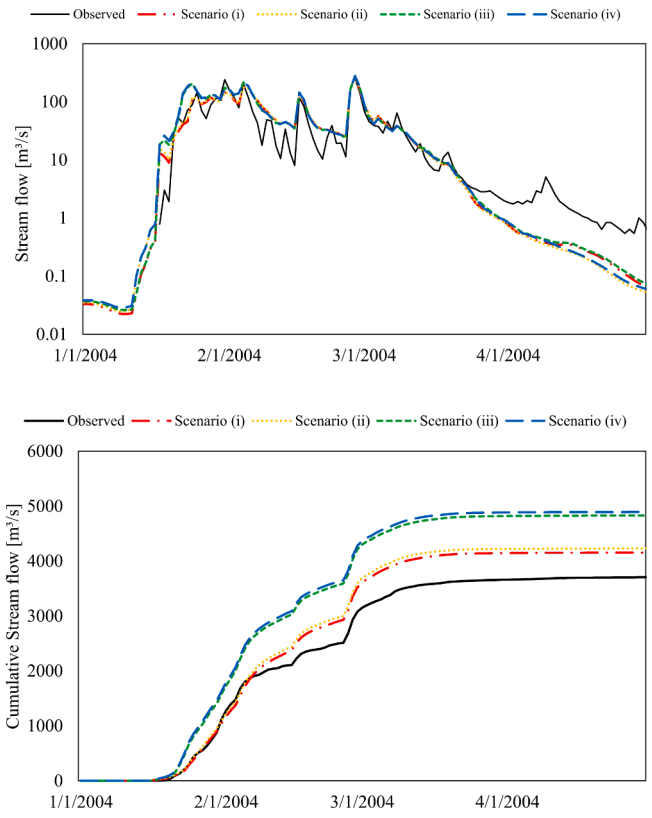

Fig. 11. Hydrographs and cumulative stream flow at Malhada station showing observed values and 4 scenarios of reservoirs during the year of 2004: scenario (i) considering all strategic reservoirs and small reservoirs (reference); (ii) removing all small reservoirs in the hydrological system, but keeping only the strategic reservoirs; (iii) removing all strategic reservoirs but keeping only the small reservoirs; (iv) removing all reservoirs.

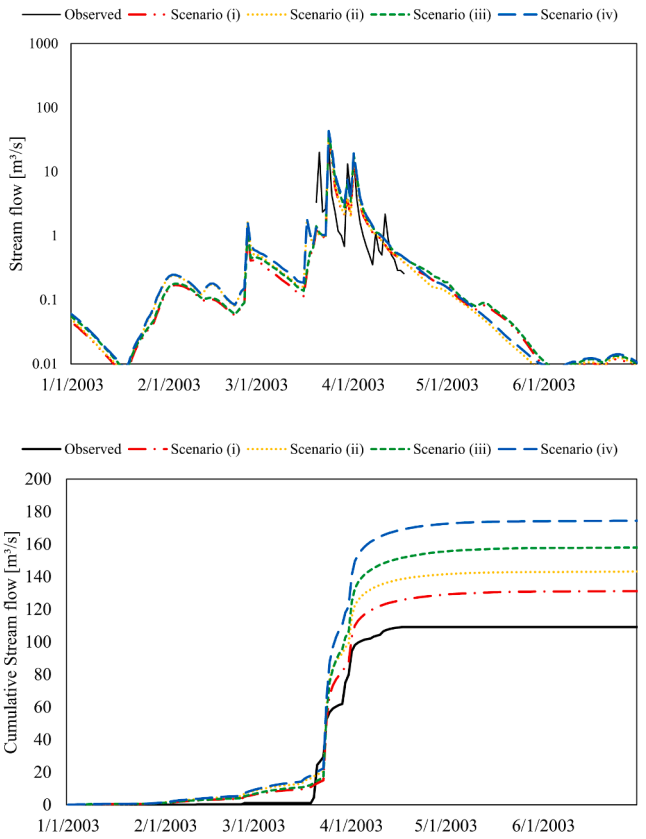

Fig. 12. Hydrographs and cumulative stream flow at Malhada station showing observed values and 4 scenarios of reservoirs during the year of 2003: scenario (i) considering all strategic reservoirs and small reservoirs (reference); (ii) removing all small reservoirs in the hydrological system, but keeping only the strategic reservoirs; (iii) removing all strategic reservoirs but keeping only the small reservoirs; (iv) removing all reservoirs.

To illustrate the results obtained for dry years with low flows, the year of 2003 was chosen to show the comparison between the simulations and the observed data, with the streamflow in the outlet at logarithmic scale (Fig. 12). The results were very similar to those obtained for wet years. All scenarios overestimate the observed streamflow data. However, the differences between scenarios (i) and (ii) and between scenarios (iii) and (iv) showed that the presence of small reservoirs is more significant for reducing the cumulative streamflow during a dry year. The water retention due to small reservoirs in dry years was 9%. Other studies have also shown that small reservoirs decrease low flows, with a more intense reduction in dry years (Perrin et al., 2012; Habets et al., 2018).

Now, modifying the dimensions of the small reservoirs ten times, we found a lower streamflow peak for the estimation with small reservoirs parameters ten times larger than the reference (original parameterization). This result was expected, because with more small reservoirs in the catchment, more water retention is observed, which means less outflow to the Malhada station. Despite this, the comparison of scenario simulations (the absence of small reservoirs, the reference and the larger dimensions of small reservoirs) for peak flow, increasing and decreasing limb were very close, with no considerable differences between the model scenarios for small reservoirs, even in dry years (not shown here).

The analysis of the reservoir volumes for the scenarios was carried out by a comparison of the time series of the storage volumes (Figs. 13–15). The results showed a small difference for the storage volume in the Poço da Pedra reservoir (Fig. 13) considering the changes in the dimensions of the small reservoirs. For the Benguê and Do Coronel reservoirs (Figs. 14 and 15, respectively), the differences in the storage volume can be observed more clearly between 2002 and 2004, with larger volumes for the "0 times" simulation, which means the absence of small reservoirs, and slightly smaller volumes for the "10 times" simulation. Once again, this was an expected result, because by decreasing the small reservoirs more water can reach the strategic reservoirs, increasing the storage volumes. However, the differences between the simulations were not considerable to conclude for a relevant impact of small reservoirs on those catchments.

Previous studies suggest a relatively high impact of small reservoirs on the catchment water retention - from 10% to 20% (de Araújo and Medeiros, 2013; Peter et al., 2014; Mamede et al., 2018; Habets et al., 2018), while the present model with new representation of small reservoirs in SWAT showed a lower impact on the water inflow for strategic reservoirs (about 2% of water retention in wet years and about 9% in dry years). The study basin has an estimate of 230 reservoirs distributed over a total catchment area of 3,347 km^2, resulting in 1 reservoir per 14.5 km^2 (reservoir density). For semi-arid regions, the variability of spatial distribution and density of small reservoirs varies significantly, between 0 and 4.2 reservoirs per km^2 (Mady et al., 2020). In comparison with other dryland regions, the Conceição River Catchment reservoir density is 25 times bigger than reservoir density in California, USA, as reported by Minear and Kondolf (2009), for example. Despite the large number of reservoirs in the Upper Jaguaribe Basin (UJB), where the study area is located, we found a reservoir density 2.5 times smaller than that of the whole UJB, which is 1 reservoir per 6 km^2 (Lima Neto et al., 2011). This indicates that the study area can still be considered to have a high density of reservoirs, although it has a lower reservoir density than the average of the UJB.

Furthermore, considering the observed data from 1979 to 2010, the

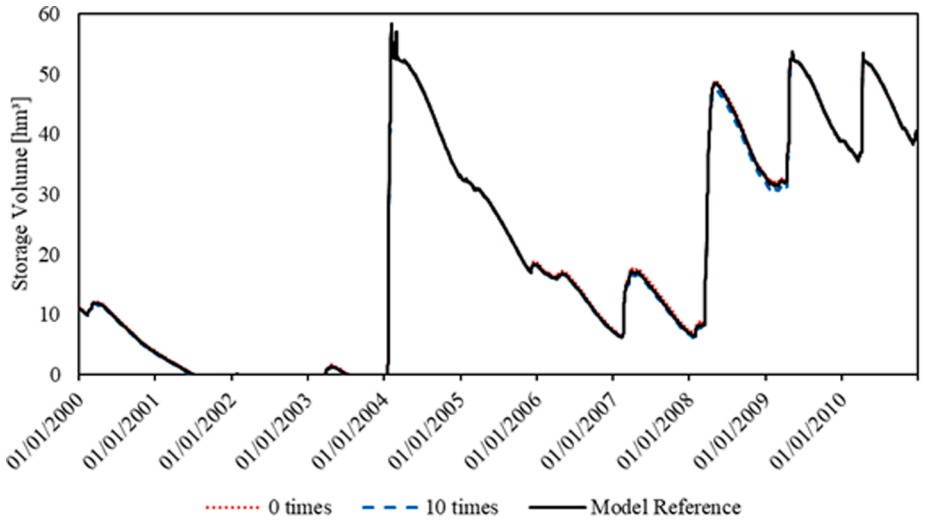

Fig. 13. Comparison for storage volumes in Poço da Pedra (2000–2010) with modifications in the dimensions of the small reservoirs in 0 and 10 times. "0 times" means the total absence of small reservoirs. "10 times" means a ten times increase in the parameters that represent the volumes of these small reservoirs. Model reference means the original parameterization.

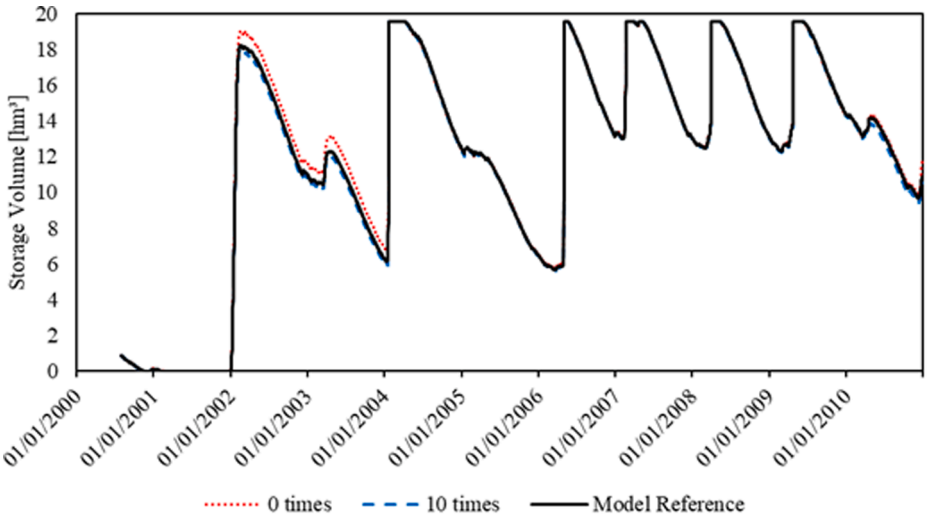

Fig. 14. Comparison for storage volumes in Benguê (2000–2010) with modifications in the dimensions of the small reservoirs in 0 and 10 times. "0 times" means the total absence of small reservoirs. "10 times" means a ten times increase in the parameters that represent the volumes of these small reservoirs. Model reference means the original parameterization.

main hydrologic fluxes of the study are: annual precipitation, annual potential evapotranspiration and annual streamflow of 605 mm, 2,328 mm and 67.8 hm^3/year (20.3 mm), respectively. The total estimated reservoir capacity is 113.1 hm^3 (or 33.8 mm), of which 94.0 hm^3 (28.1 mm) comes from three strategic reservoirs. Ponds and main private reservoirs (226) have only 19.1 hm^3 (5.7 mm), on average 0.085 hm^3 (0.025 mm) per small reservoir. Even increasing the volume estimates of small reservoirs by ten times, the average volume per area of each small reservoir (0.25 mm) remains very small in comparison with strategic reservoirs and the aforementioned hydrologic fluxes. Moreover, as the stream flow are normally concentrated in a few days of the year in this catchment, the surface runoff has much more volume than the capacity of the small reservoirs, even for forcing moderate rainfall events.

Although the results obtained in this work represent hydrological aspects of a specific catchment in the Brazilian semiarid region, the methodology for assessing the impact of small reservoirs and the discussion of hydrological processes, such as peak flow and non-flow periods, channel transmission losses, analysis at the beginning and end of the rainy season in the streamflow gauge station hydrographs and in the storage volume of reservoirs, as well as the parameterization of the dense network of reservoirs, can also be applied to large-scale catchments located in other dryland regions. Some examples include semiarid watersheds in Australia, United States, Mexico and South Asia, which present similar climate, hydrological and land-use characteristics.

5. Conclusions

In this study, we assessed the impact of small reservoirs on a dryland catchment with a high-density network of reservoirs and investigated the water routing dynamics and hydrological processes in the basin. For this purpose, a model was developed to simulate the catchment streamflow at the outlet, the storage volumes of large reservoirs and the water balance of lumped small-reservoirs at sub-basin scale. A methodology for the parameterization of the small reservoirs was developed to represent their integration into the catchment hydrological modeling and to investigate their influence on the hydrological outputs (streamflow and reservoir volume storage) of the basin.

The main findings of our work can be described as follows:

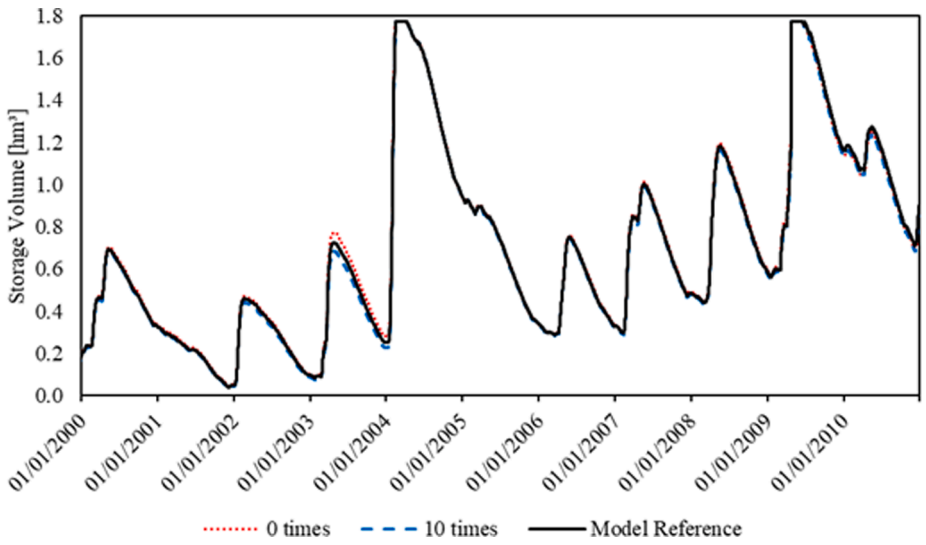

Fig. 15. Comparison for storage volumes in Do Coronel (2000–2010) with modifications in the dimensions of the small reservoirs in 0 and 10 times. "0 times" means the total absence of small reservoirs. "10 times" means a ten times increase in the parameters that represent the volumes of these small reservoirs. Model reference means the original parameterization.

1. The model proved to be well suited for simulating peak flow in wet years, the non-flow periods and the rising limb of the hydrograph with high reliability for the streamflow at the catchment outlet.
2. In the strategic reservoirs, wet and dry years were well represented, as well as the magnitude of spillway overflow of strategic and small reservoirs. On the other hand, the number of days with spillway overflow showed to be overestimated.
3. The proposed model presents an innovative way to represent a dense network of reservoirs in semi-arid basins in catchment hydrological models. The efforts in the parameterization and aggregation of ponds and reservoirs proved to be worthwhile, allowing a more accurate spatial representation of the strategic and small reservoirs in the SWAT model for high-density networks and improving the analysis of the hydrological processes and impacts in the basin.
4. The presence of small reservoirs decreased the stream flow and storage downstream reservoir volumes, with only 2% of water retention on average. Increasing the volumes of small reservoirs along the basin by ten times showed that the small ponds had a low influence on stream discharge. The catchment under study is far from reaching its maximum water reserve capacity, especially considering the current density of small reservoirs. However, in dry years, their impact can reach 9% of water retention, which may worsen periods of water scarcity in the large reservoirs.

For semi-arid catchments, the reliability of the results for peak flow in wet years, for non-flow periods and for the rising limb of the hydrograph is very important for the simulation of the stream flow reaching the large reservoirs and, consequently, for meeting the water demand at catchment scale. However future improvements should be done in the model for better representations in recession flow.

Since the results of the present study pointed to a low influence of the network of small reservoirs on the stream flow and strategic reservoir storages, the small reservoirs in the catchment might be an option to increase decentralized water access for small rural communities, without competing with other water uses, such as large and medium-sized city sanitation demands and irrigation industry, from the strategic reservoirs.

The spatial representation of small reservoirs for a high-density network in the SWAT model and the results of the cumulative impact of small reservoirs presented in this study contributed to a better understanding of hydrology in dryland catchments, and can be applied to catchments in similar climatic and socio-economic environments. Further studies on the SWAT model in semi-arid regions will evaluate different arrangements for the increase of small reservoirs in the basin and their impact on reservoir water quality. Such studies should also be concerned with investigating channel transmission losses and river-aquifer interactions, based on comparison with additional (intermittent) groundwater data. The coupling of surface and groundwater models will potentially improve the understanding of dryland hydrology and integrated water resources management in semi-arid regions.

CRediT authorship contribution statement

Udinart Prata Rabelo: Validation, Formal analysis, Visualization, Investigation, Data curation, Writing – original draft. **Jörg Dietrich:** Supervision, Conceptualization, Methodology, Writing – original draft, Writing – review & editing. **Alexandre Cunha Costa:** Supervision, Conceptualization, Methodology, Writing – original draft, Writing – review & editing, Resources. **Max Nino Simshäuser:** Investigation, Formal analysis, Methodology, Writing – original draft. **Fernanda Elise Scholz:** Investigation, Formal analysis. **Tam V. Nguyen:** Formal analysis, Software, Supervision. **Iran Eduardo Lima Neto:** Writing – review & editing, Supervision, Conceptualization.

Declaration of Competing Interest

The authors declare that they have no known competing financial interests or personal relationships that could have appeared to influence the work reported in this paper.

Acknowledgements

We would like to thank the Foundation for Meteorology and Water Resources of the State of Ceará (FUNCEME) for making available the DEM, the raw information about the landscape properties and the meteorological time series and the Deutscher Akademischer Austauschdienst (DAAD) for supporting field work. We also thank the Water Agency of the State of Ceará (COGERH) and the Secretary of Water Resources of the government of Ceará (SRH) for providing reservoir data. Finally, we are grateful for the streamflow time series, which were made available by the Brazilian Water Agency (ANA).

Funding

This study was supported by the Foundation for Scientific and Technological Development of the State of Ceará (FUNCAP) (PNE0112–00042.01.00/16), the Brazilian National Council for Scientific and Technologica Development (CNPq) (155814/2018–4) and by Deutscher Akademischer Austauschdienst (DAAD).

Appendix A. Supplementary data

Supplementary data to this article can be found online at https://doi.org/10.1016/j.jhydrol.2021.127103.

References

Abouabdillah, A., White, M., Arnold, J.G., De Girolamo, A.M., Oueslati, O., Maataoui, A., Lo Porto, A., 2014. Evaluation of soil and water conservation measures in a semi-arid river basin in Tunisia using SWAT. Soil Use Manag. 30 (4), 539–549. https://doi.org/10.1111/sum.2014.30.issue-410.1111/sum.12146.

AghaKouchak, A., Feldman, D., Hoerling, M., Huxman, T., Lund, J., 2015. Water and climate: Recognize anthropogenic drought. Nature 2015 5247566 524, 409–411. https://doi.org/10.1038/524409a.

Aigner, D., 2008. Dresdner Wasserbauliche Mitteilungen Heft 36. Überfälle. Edited by Technische Universität Dresden. Dresden. Available online at http://rcswww.urz.tu-dresden.de/~daigner/pdf/ueberf.pdf.

Andaryani, S., Trolle, D., Nikjoo, M.R., Moghadam, M.H.R., Mokhtari, D., 2019. Forecasting near-future impacts of land use and climate change on the Zilbier river hydrological regime, northwestern Iran. Environ. Earth Sci. 78, 1–14. https://doi.org/10.1007/s12665-019-8193-4.

Andrade, C.W.L.d., Montenegro, S.M.G.L., Montenegro, A.A.A., Lima, J.R.d.S., Srinivasan, R., Jones, C.A., 2019. Soil moisture and discharge modeling in a representative watershed in northeastern Brazil using SWAT. Ecohydrol. Hydrobiol. 19 (2), 238–251. https://doi.org/10.1016/j.ecohyd.2018.09.002.

de Araújo, J.C., Medeiros, P.H.A., 2013. Impact of Dense Reservoir Networks on Water Resources in Semiarid Environments. Australas. J. Water Resour. 17 (1), 87–100. https://doi.org/10.7158/13241583.2013.11465422.

Arnold, J.G., Moriasi, D.N., Gassman, P.W., Abbaspour, K.C., White, M.J., Srinivasan, R., Santhi, C., Harmel, R.D., van Griensven, A., Van Liew, M.W., Kannan, N., Jha, M.K., 2012. SWAT: Model Use, Calibration, and Validation. Trans. ASABE 55, 1491–1508. https://doi.org/10.13031/2013.42256.

Attarod, P., Sadeghi, S.M.M., Pypker, T.G., Bagheri, H., Bagheri, M., Bayramzadeh, V., 2015. Needle-leaved trees impacts on rainfall interception and canopy storage capacity in an arid environment. New For. 46 (3), 339–355. https://doi.org/10.1007/s11056-014-9464-2.

Ayalew, T.B., Krajewski, W.F., Mantilla, R., Wright, D.B., Small, S.J., 2017. Effect of Spatially Distributed Small Dams on Flood Frequency: Insights from the Soap Creek Watershed. J. Hydrol. Eng. 22 (7), 04017011. https://doi.org/10.1061/(ASCE)HE.1943-5584.0001513.

Berg, M.D., Popescu, S.C., Wilcox, B.P., Angerer, J.P., Rhodes, E.C., McAlister, J., Fox, W. E., 2016. Small farm ponds: overlooked features with important impacts on watershed sediment transport. JAWRA J. Am. Water Resour. Assoc. 52 (1), 67–76. https://doi.org/10.1111/1752-1688.12369.

Berhane, G., Gebreyohannes, T., Martens, K., Walraevens, K., 2016. Overview of micro-dam reservoirs (MDR) in Tigray (northern Ethiopia): Challenges and benefits. J. African Earth Sci. 123, 210–222. https://doi.org/10.1016/J.JAFREARSCI.2016.07.022.

Bressiani, D.A., Gassman, P.W., Fernandes, J.G., Hamilton, L., Garbossa, P., Srinivasan, R., Bonumá, N.B., Mendiondo, E.M., 2015. Review of Soil and Water Assessment Tool (SWAT) applications in Brazil: challenges and prospects. Int. J. Agric. Biol. Eng. 8, 9–35. https://doi.org/10.25165/ijabe.v8i3.1765.

Bronstert, A., de Araújo, J.-C., Batalla, R.J., Costa, A.C., Delgado, J.M., Francke, T., Foerster, S., Guentner, A., López-Tarazón, J.A., Mamede, G.L., Medeiros, P.H., Mueller, E., Vericat, D., 2014. Process-based modelling of erosion, sediment transport and reservoir siltation in mesoscale semi-arid catchments. J. Soils Sediments 2014 1412 14, 2001–2018. https://doi.org/10.1007/S11368-014-0994-1.

Callow, J.N., Smettem, K.R.J., 2009. The effect of farm dams and constructed banks on hydrologic connectivity and runoff estimation in agricultural landscapes. Environ. Model. Softw. 24 (8), 959–968. https://doi.org/10.1016/j.envsoft.2009.02.003.

Carluer, N., Babut, M., Belliard, J., Bernez, I., Burger-Leenhardt, D., Dorioz, J.M., Douez, O., Dufour, S., Grimaldi, C., Habets, F., Le Bissonnais, Y., Molénat, J., Rollet, A.J., Rosset, V., Sauvage, S., Usseglio-Polatera, P., Leblanc, B., 2016. Expertise scientifique collective sur l'impact cumulé des retenues. Rapport de synthèse. 82 pp + annexes.

Colares, J.Q.d.S., Feitosa F.A.C., 1998. Diagnóstico do Município de Campos Sales. Edited by Ministério de Minas e Energia, Serviço Geológico do Brasil. Fortaleza (Programa de Recenseamento de Fontes de Abastecimento por Água Subterrânea no Estado do Ceará).

Costa, A.C., Bronstert, A., De Araújo, J.C., 2012. A channel transmission losses model for different dryland rivers. Hydrol. Earth Syst. Sci. 16, 1111–1135. https://doi.org/10.5194/hess-16-1111-2012.

Costa, Alexandre Cunha, Foerster, Saskia, de Araújo, José Carlos, Bronstert, Axel, 2013. Analysis of channel transmission losses in a dryland river reach in north-eastern Brazil using streamflow series, groundwater level series and multi-temporal satellite data. Hydrol. Process. 27 (7), 1046–1060. https://doi.org/10.1002/hyp.v27.710.1002/hyp.9243.

Daggupati, P., Pai, N., Ale, S., Douglas-Mankin, K.R., Zeckoski, R.W., Jeong, J., Parajuli, P.B., Saraswat, D., Youssef, M.A., 2015. A Recommended Calibration and Validation Strategy for Hydrologic and Water Quality Models. Trans. ASABE 58, 1705–1719. https://doi.org/10.13031/TRANS.58.10712.

de Figueiredo, José Vidal, de Araújo, José Carlos, Medeiros, Pedro Henrique Augusto, Costa, Alexandre C., 2016. Runoff initiation in a preserved semiarid Caatinga small watershed, Northeastern Brazil. Hydrol. Process. 30 (13), 2390–2400. https://doi.org/10.1002/hyp.v30.1310.1002/hyp.10801.

Eudoro, W.S., 2009. Caderno Regional da Sub-bacia do Alto Jaguaribe. Edited by Assembleia Legislativa do Estado, Conselho de Altos Estudos e Assuntos Estratégicos. INESP. Fortaleza, CE (Coleção Cadernos Regionais do Pacto das Águas 5.

Feitosa, F.A.C., 1998. Diagnóstico do Município de Aiuaba. Edited by Ministério de Minas e Energia, Serviço Geológico do Brasil. Fortaleza (Programa de Recenseamento de Fontes de Abastecimento por Água Subterrânea no Estado do Ceará).

Feitosa, F.A.C., Oliveira, F.V.C. de, 1998. Diagnóstico do Município de Salitre. Edited by Ministério de Minas e Energia, Serviço Geológico do Brasil. Fortaleza (Programa de Recenseamento de Fontes de Abastecimento por Água Subterrânea no Estado do Ceará).

Fowe, T., Karambiri, H., Paturel, J.E., Poussin, J.C., Cecchi, P., 2015. Water balance of small reservoirs in the volta basin: A case study of boura reservoir in burkina faso. Agric. Water Manag. 152, 99–109. https://doi.org/10.1016/j.agwat.2015.01.006.

Fowler, K., Morden, R., Lowe, L., Nathan, R., 2016. Advances in assessing the impact of hillside farm dams on streamflow. https://doi.org/10.1080/13241583.2015.1116182 19, 96–108. https://doi.org/10.1080/13241583.2015.1116182.

Gatto, L.C.S., 1999. Diagnóstico Ambiental da Bacia do Rio Jaguaribe. Diretrizes Gerais para a Ordenação Territorial. 1st ed. Edited by Funcação Instituto Brasileiro de Geografia e Estatística, IBGE, Diretoria Geociências. Ministério de Planejamento e Orçâmento. Salvador (DIGEO, 1).

Ghoraba, Shimaa M., 2015. Hydrological modeling of the Simly Dam watershed (Pakistan) using GIS and SWAT model. Alexandria Eng. J. 54 (3), 583–594. https://doi.org/10.1016/j.aej.2015.05.018.

Güntner, A., 2002. Large-Scale Hydrological Modelling in the Semi-Arid North-East of Brazil. Dissertation. University of Potsdam, Potsdam. Department of Geoecology.

Güntner, Andreas, Krol, Maarten S., Araújo, José Carlos De, Bronstert, Axel, 2004. Simple water balance modelling of surface reservoir systems in a large data-scarce semiarid region / Modélisation simple du bilan hydrologique de systèmes de réservoirs de surface dans une grande région semi-aride pauvre en données. Hydrol. Sci. J. 49 (5) https://doi.org/10.1623/hysj.49.5.901.55139.

Gutiérrez, A.P.A., Engle, N.L., De Nys, E., Molejón, C., Martins, E.S., 2014. Drought preparedness in Brazil. Weather Clim. Extrem. 3, 95–106. https://doi.org/10.1016/j.wace.2013.12.001.

Habets, F., Molénat, J., Carluer, N., Douez, O., Leenhardt, D., 2018. The cumulative impacts of small reservoirs on hydrology: A review. Sci. Total Environ. 643, 850–867. https://doi.org/10.1016/J.SCITOTENV.2018.06.188.

Hughes, D.A., Mantel, S.K., 2010. Estimating the uncertainty in simulating the impacts of small farm dams on streamflow regimes in South Africa. Hydrol. Sci. J. 55 (4), 578–592. https://doi.org/10.1080/02626667.2010.484903.

Jajarmizadeh, M., Sidek, L.M., Harun, S., Salarpour, M., 2017. Optimal Calibration and Uncertainty Analysis of SWAT for an Arid Climate: https://doi.org/10.1177/1178622117731792.

Kim, K.B., Kwon, H.H., Han, D., 2018. Exploration of warm-up period in conceptual hydrological modelling. J. Hydrol. 556, 194–210. https://doi.org/10.1016/J.JHYDROL.2017.11.015.

Lima Neto, Iran Eduardo, Wiegand, Mário Cesar, de Araújo, José Carlos, 2011. Sediment redistribution due to a dense reservoir network in a large semi-arid Brazilian basin. Hydrol. Sci. J. 56 (2), 319–333. https://doi.org/10.1080/02626667.2011.553616.

Liu, Yongbo, Yang, Wanhong, Yu, Zhiqiang, Lung, Ivana, Yarotski, Jim, Elliott, Jane, Tiessen, Kevin, 2014. Assessing Effects of Small Dams on Stream Flow and Water Quality in an Agricultural Watershed. J. Hydrol. Eng. 19 (10), 05014015. https://doi.org/10.1061/(ASCE)HE.1943-5584.0001005.

Luo, Kaisheng, Tao, Fulu, Deng, Xiangzheng, Moiwo, Juana P., 2017. Changes in potential evapotranspiration and surface runoff in 1981–2010 and the driving factors in Upper Heihe River Basin in Northwest China. Hydrol. Process. 31 (1), 90–103. https://doi.org/10.1002/hyp.v31.110.1002/hyp.10974.

Mady, Bassem, Lehmann, Peter, Gorelick, Steven M, Or, Dani, 2020. Distribution of small seasonal reservoirs in semi-arid regions and associated evaporative losses. Environ. Res. Commun. 2 (6), 061002. https://doi.org/10.1088/2515-7620/ab92af.

Mallakpour, I., Sadegh, M., Aghakouchak, A., 2018. A new normal for streamflow in California in a warming climate: Wetter wet seasons and drier dry seasons. J. Hydrol. 567, 203–211. https://doi.org/10.1016/j.jhydrol.2018.10.023.

Malveira, Vanda Tereza Costa, Araújo, José Carlos de, Güntner, Andreas, 2012. Hydrological Impact of a High-Density Reservoir Network in Semiarid Northeastern Brazil. J. Hydrol. Eng. 17 (1), 109–117. https://doi.org/10.1061/(ASCE)HE.1943-5584.0000404.

Mamede, G.L., Araujo, N.A.M., Schneider, C.M., de Araujo, J.C., Herrmann, H.J., 2012. Overspill avalanching in a dense reservoir network. Proc. Natl. Acad. Sci. U. S. A. 109 (19), 7191–7195. https://doi.org/10.1073/pnas.1200398109.

Mamede, George L., Guentner, Andreas, Medeiros, Pedro H.A., de Araújo, José Carlos, Bronstert, Axel, 2018. Modeling the Effect of Multiple Reservoirs on Water and

Sediment Dynamics in a Semiarid Catchment in Brazil. J. Hydrol. Eng. 23 (12), 05018020. https://doi.org/10.1061/(ASCE)HE.1943-5584.0001701.
Mendoza, J.A.C., Alcazar, T.A.C., Medina, S.A.Z., 2021. Calibration and Uncertainty Analysis for Modelling Runoff in the Tambo River Basin, Peru, Using Sequential Uncertainty Fitting Ver-2 (SUFI-2) Algorithm. https://doi.org/10.1177/1178622120988707.
Mengistu, Achamyeleh G., van Rensburg, Leon D., Woyessa, Yali E., 2019. Techniques for calibration and validation of SWAT model in data scarce arid and semi-arid catchments in South Africa. J. Hydrol. Reg. Stud. 25, 100621. https://doi.org/10.1016/j.ejrh.2019.100621.
Minear, J. Toby, Kondolf, G. Matt, 2009. Estimating reservoir sedimentation rates at large spatial and temporal scales: A case study of California. Water Resour. Res. 45 (12) https://doi.org/10.1029/2007WR006703.
Molina-Navarro, E., Hallack-Alegría, M., Martínez-Pérez, S., Ramírez-Hernández, J., Mungaray-Moctezuma, A., Sastre-Merlín, A., 2016. Hydrological modeling and climate change impacts in an agricultural semiarid region. Case study: Guadalupe River basin, Mexico. Agric. Water Manag. 175, 29–42. https://doi.org/10.1016/j.agwat.2015.10.029.
Molle, F., 1989. Perdas por Evaporação e Infiltração em Pequenos Açudes. 2nd ed. Edited by Superintendência do Desenvolvimento do Nordeste. SUDENE/ORSTOM (TAPI). Recife, PE (Série Hidrologia, 25). Available online at http://horizon.documentation.ird.fr/exldoc/pleins_textes/pleins_textes_7/b_fdi_03_01/33854.pdf.
Molle, F., 1994. Geometria Dos Pequenos Açudes. 2nd ed. Edited by Superintendência do Desenvolvimento do Nordeste. SUDENE/ORSTOM (TAPI). Recife, PE (Série Hidrologia, 29). Available online at http://horizon.documentation.ird.fr/exl-doc/pleins_textes/pleins_textes_7/divers2/010033411.pdf.
Nascimento, Antônia Tatiana Pinheiro do, Cavalcanti, Natália Holanda Maia, Castro, Bruno Parente Leitão de, Medeiros, Pedro Henrique Augusto, 2019. Decentralized water supply by reservoir network reduces power demand for water distribution in a semi-arid basin. Hydrol. Sci. J. 64 (1), 80–91. https://doi.org/10.1080/02626667.2019.1566728.
Nathan, Rory, Jordan, Phillip, Morden, Robert, 2005. Assessing the impact of farm dams on streamflows, Part I: Development of simulation tools. Australas. J. Water Resour. 9 (1), 1–12. https://doi.org/10.1080/13241583.2005.11465259.
Nathan, R., Lowe, L., 2012. The Hydrologic Impacts of Farm Dams. Australas J. Water Resour. 16 (1), 75–83. https://doi.org/10.7158/13241583.2012.11465405.
Neal, B., Nathan, R.J., Schreider, S., Jakeman, A.J., 2002. Identifying the Separate Impact of Farm Dams and Land Use Changes on Catchment Yield. Australas. J. Water Resour. 5 (2), 165–176. https://doi.org/10.1080/13241583.2002.11465202.
Neitsch, S.L., Arnold, J.G., Kiniry, J.R., Williams J.R., 2009. Soil and Water Assessment Tool. Theoretical Documentation. Version 2009. Edited by Texas Water Resource Institute: Grassland, Soil and Water Research Laboratory - Agricultural Research Service, Blackland Research Center - Texas AgriLife Research. Texas A&M University System. College Station, Texas (Texas Water Resources Institute Technical Report, 406). Available online at http://swat.tamu.edu/media/99192/swat2009-theory.pdf.
Nguyen, H.H., Recknagel, F., Meyer, W., Frizenschaf, J., 2017. Analysing the Effects of Forest Cover and Irrigation Farm Dams on Streamflows of Water-Scarce Catchments in South Australia through the SWAT Model. Water 2017, Vol. 9, Page 33 9, 33. https://doi.org/10.3390/W9010033.
Nguyen, V., Dietrich, J., Uniyal, B., Tran, D., 2018. Verification and Correction of the Hydrologic Routing in the Soil and Water Assessment Tool. Water 10, 1419. https://doi.org/10.3390/w10101419.
Paredes-Beltran, B., Sordo-Ward, A., Garrote, L., 2021. Dataset of Georeferenced Dams in South America (DDSA). Earth Syst. Sci. Data 13, 213–229. https://doi.org/10.5194/ESSD-13-213-2021.
Pereira, B.S., 2017. Estimativa de Volumes de Reservatórios de Região Semiárida com Alta Densidade de Resevatórios por Sensoriamento Remoto. Dissertation. Instituto Federal de Educação, Ciência e Tecnologia do Ceará, Fortaleza, CE. Departamento de Planejamento, Orçamento e Gestão.
Perrin, J., Ferrant, S., Massuel, S., Dewandel, B., Maréchal, J.C., Aulong, S., Ahmed, S., 2012. Assessing water availability in a semi-arid watershed of southern India using a semi-distributed model. J. Hydrol. 460–461, 143–155. https://doi.org/10.1016/J.JHYDROL.2012.07.002.
Peter, S.J., de Araújo, J.C., Araújo, N.A.M., Herrmann, H.J., 2014. Flood avalanches in a semiarid basin with a dense reservoir network. J. Hydrol. 512, 408–420. https://doi.org/10.1016/j.jhydrol.2014.03.001.
Pinheiro, F.D., 2004. Açudagem particular em cooperação no Ceará, Série conViver, 732 p. Departamento Nacional de Obras Contra a Seca (DNOCS).
Rödiger, T., Geyer, S., Mallast, U., Merz, R., Krause, P., Fischer, C., Siebert, C., 2014. Multi-response calibration of a conceptual hydrological model in the semiarid catchment of Wadi al Arab. Jordan. J. Hydrol. 509, 193–206. https://doi.org/10.1016/J.JHYDROL.2013.11.026.
Samimi, Maryam, Mirchi, Ali, Moriasi, Daniel, Ahn, Sora, Alian, Sara, Taghvaeian, Saleh, Sheng, Zhuping, 2020. Modeling arid/semi-arid irrigated agricultural watersheds with SWAT: Applications, challenges, and solution strategies. J. Hydrol. 590, 125418. https://doi.org/10.1016/j.jhydrol.2020.125418.
Santos, C., Almeida, C., Ramos, T., Rocha, F., Oliveira, R., Neves, R., 2018. Using a Hierarchical Approach to Calibrate SWAT and Predict the Semi-Arid Hydrologic Regime of Northeastern Brazil. Water 10, 1137. https://doi.org/10.3390/w10091137.
Schreider, S.Yu., Jakeman, A.J., Letcher, R.A., Nathan, R.J., Neal, B.P., Beavis, S.G., 2002. Detecting changes in streamflow response to changes in non-climatic catchment conditions: Farm dam development in the Murray-Darling basin. Australia. J. Hydrol. 262 (1-4), 84–98. https://doi.org/10.1016/S0022-1694(02)00023-9.
Silva, F.J.A., Araújo, A.L., Souza, R.O., 2007. Águas subterrâneas no Ceará - poços instalados e salinidade. In Revista Tecnologica Fortaleza (UNIFOR) 28 (2), 136–159.
Simmers, I., 2003. In: Understanding water in a dry environment. Hydrological processes in arid and semi-arid zones. A.A. Balkema (International contributions to hydrogeology, Lisse, Abingdon, p. 23)..
Siqueira, M.S., de Alcântara, H.M., Ribeiro, G.N., Medeiros, P.C., Afonso, J.P.S.D., de Medeiros, A.C., Maracajá, P.B., 2016. Influence of the scale effect on the sediment yield in not instrumented basins in the semiarid zone. Revista Brasileira de Gestão Ambiental 11 (01), 99–105.
Sukhbaatar, Chinzorig, Sajjad, Raja Umer, Lunten, Janchivdorj, Yu, Seung-Hoon, Lee, Chang-Hee, 2017. Climate Change Impact on the Tuul River Flow in a Semiarid Region in Mongolia. Water Environ. Res. 89 (6), 527–538. https://doi.org/10.2175/106143016X14798353399223.
Sun, L., Yang, L., Hao, L., Fang, D., Jin, K., Huang, X., 2017. Hydrological Effects of Vegetation Cover Degradation and Environmental Implications in a Semiarid Temperate Steppe, China. Sustainability 9, 281. https://doi.org/10.3390/su9020281.
Uniyal, B., Dietrich, J., Vu, N.Q., Jha, M.K., Arumí, J.L., 2019. Simulation of regional irrigation requirement with SWAT in different agro-climatic zones driven by observed climate and two reanalysis datasets. Sci. Total Environ. 649, 846–865. https://doi.org/10.1016/j.scitotenv.2018.08.248.
Yaeger, M.A., Reba, M.L., Massey, J.H., Adviento-Borbe, M.A.A., 2017. On-Farm Irrigation Reservoirs in Two Arkansas Critical Groundwater Regions: A Comparative Inventory. Appl. Eng. Agric. 33, 869–878. https://doi.org/10.13031/AEA.12352.
Yao, J., Liu, H., Huang, J., Gao, Z., Wang, G., Li, D., Yu, H., Chen, X., 2020. Accelerated dryland expansion regulates future variability in dryland gross primary production. Nat. Commun. 2020 111 11, 1–10. https://doi.org/10.1038/s41467-020-15515-2.
Zettam, A., Taleb, A., Sauvage, S., Boithias, L., Belaidi, N., Sánchez-Pérez, J., 2017. Modelling Hydrology and Sediment Transport in a Semi-Arid and Anthropized Catchment Using the SWAT Model: The Case of the Tafna River (Northwest Algeria). Water 9, 216. https://doi.org/10.3390/w9030216.
Zhang, C., Peng, Y., Chu, J., Shoemaker, C.A., Zhang, A., 2012. Integrated hydrological modelling of small-and medium-sized water storages with application to the upper fengman reservoir basin of China. Hydrol. Earth Syst. Sci. 16, 4033–4047. https://doi.org/10.5194/hess-16-4033-2012.
Zhang, S., Foerster, S., Medeiros, P., de Araújo, J.C., Motagh, M., Waske, B., 2016. Bathymetric survey of water reservoirs in north-eastern Brazil based on TanDEM-X satellite data. Sci. Total Environ. 571, 575–593. https://doi.org/10.1016/j.scitotenv.2016.07.0.
Zhang, Zhenyu, Liu, Jihui, Huang, Jinliang, 2020. Hydrologic impacts of cascade dams in a small headwater watershed under climate variability. J. Hydrol. 590, 125426. https://doi.org/10.1016/j.jhydrol.2020.125426.